THESIS

TECHNO-ECONOMIC ANALYSIS AND LIFE CYCLE ASSESSMENT OF ALGAL TURF SCRUBBERS TREATING WASTEWATER EFFLUENT FOR RENEWABLE DIESEL PRODUCTION

Submitted by

Ashley Ryland

Department of Mechanical Engineering

In partial fulfillment of the requirements

For the Degree of Master of Science

Colorado State University

Fort Collins, Colorado

Summer 2025

Master's Committee:

Advisor: Jason Quinn

Kenneth Reardon
Reza Nazemi

ABSTRACT

TECHNO-ECONOMIC ANALYSIS AND LIFE CYCLE ASSESSMENT OF ALGAL TURF SCRUBBERS TREATING WASTEWATER EFFLUENT FOR RENEWABLE DIESEL PRODUCTION

Algal turf scrubbers (ATS) are a promising wastewater treatment technology that can simultaneously remove nutrients from effluent and generate algal biomass for conversion into renewable fuels. This study presents the first integrated techno-economic analysis (TEA) and life cycle assessment (LCA) of ATS systems treating effluent from point-source wastewater treatment plants across the continental United States. A regionally resolved process model was developed using watershed data to simulate nutrient removal and biomass production, with biomass subsequently routed to centralized biorefineries for conversion to renewable diesel via hydrothermal liquefaction. The analysis incorporates non-co-located infrastructure and average transportation distances to reflect real-word deployment logistics. Economic viability was evaluated using a discounted cash flow rate of return model, and environmental impacts were assessed using a well-to-wheels LCA framework. Moreover, the TEA incorporates differentiated nutrient credits for nitrogen and phosphorus removal, enabling a more accurate evaluation of water quality services. Results indicate that ATS systems are effective at nutrient removal, with 75% of modeled sites achieving cost competitiveness for fuel production (< \$0.87 per liter gasoline equivalent) when nutrient credits of \$42 kg^{-1} for nitrogen and \$321 kg^{-1} for phosphorus removal are applied. However, only 29% of sites present lower life cycle greenhouse gas emissions below the renewable fuel standard (45 g CO_{2eq} MJ^{-1}), limiting locations of feasible

deployment. Nonetheless, ATS systems exhibit lower energy and carbon intensity compared to conventional tertiary treatment technologies, offering a viable pathway toward integrated wastewater management and biofuel production.

ACKNOWLEDGEMENTS

The author gratefully acknowledges financial support from the United States Department of Energy (DE-EE0008906 and DE-EE0008902). Special thanks are extended to Peter Chen at the Powerhouse Energy Institute for assisting with the experimental work that supported this study. The author also would like to acknowledge at Sungwhan Kim, Ryan Davis, and Tyler Eckles, Sandia National Laboratories, for their technical expertise, and Mark Zivojnovich for his insights on commercial-scale implementation. Gratitude is further extended to Dr. Quinn and the members of the Sustainability Research Lab at the Powerhouse Energy Institute for their ongoing support throughout this work. Finally, sincere thanks to David Quiroz for his thoughtful editing of the manuscript of the journal submission that forms the core content of this thesis.

TABLE OF CONTENTS

1. INTRODUCTION

As global decarbonization goals intensify, hard-to-electrify sectors, such as heavy-duty transportation, require low-carbon alternatives to conventional fuels. Heavy-duty transport accounts for 23% of emissions within the transportation sector, which itself represented the largest portion of total U.S. greenhouse gas emissions in 2022 [1]. Concurrently, wastewater treatment plants (WWTPs) face increasing regulatory pressure to address nutrient pollution, specifically nitrogen and phosphorus, in order to improve water quality and comply with increasingly stringent environmental standards [2]. Algal Turf Scrubbers (ATS), when integrated with WWTPs, present a viable dual-purpose approach by efficiently removing excess nutrients from effluent while generating biomass that can be converted into renewable fuels, thus supporting both water quality improvement and broader decarbonization efforts in the transportation sector.

In ATS systems, diverse algal polycultures are cultivated as biofilms on gently sloped surfaces under continuous flow. This polyculture-based configuration promotes system stability and enhances nutrient uptake due to both the complementary metabolic activity of multiple algal species and the rapid growth rates characteristic of many filamentous and turf-forming algae [3], [4], [5]. These high growth rates, often exceeding those of terrestrial crops, contribute to efficient nitrogen and phosphorus assimilation and produce nutrient-rich biomass while reducing the risk of culture collapse compared to monocultures [4]. As a result, ATS systems are particularly attractive for integration into existing WWTP infrastructure to enable simultaneous nutrient removal and biomass generation for downstream fuel production.

Despite these advantages, ATS systems have not yet been widely implemented in municipal wastewater treatment applications. However, they have shown promise in treating a variety of water sources, including surface water and wastewater [6], [7], [8], [9], [10], [11]. Several studies have demonstrated their effectiveness in nutrient removal, and a few have utilized techno-economic analysis (TEA) and life cycle assessment (LCA) to evaluate economic feasibility and environmental impacts. For instance, Banks et al. (2023) and DeRose et al. (2021) focused on the application of ATS to address nutrient pollution in surface waters, particularly for mitigating harmful algal blooms [9], [10]. In contrast, there are relatively few TEA and LCA studies evaluating ATS systems for treating point-source wastewater. Notably, in an economic and lifecycle study for ATS systems treating dairy wastewater, Higgins et al. (2012) found that implementing ATS systems ($1.42 m^{-3}) was not cost competitive with conventional treatment ($0.2 m^{-3}). The study concluded that nutrient credits of $3.83 kg^{-1} for nitrogen and $9.57 kg^{-1} for phosphorus would be required to make ATS systems economically viable. Further, Higgins et al. (2012) reported that ATS dairy wastewater treatment resulted in a GWP of -1.5 kg CO_{2eq} m^3 wastewater under low recirculation, which increased to 0.5 kg CO_{2eq} m^3 wastewater when high recirculation was applied [6]. These findings underscore that successful ATS deployment at point sources depends on nutrient credit valuation and removal efficiency, as nutrient credits strongly impact economic feasibility while recirculation requirement can greatly increase GWP. Overall, existing studies demonstrate that ATS systems can effectively treat a range of sources, though further TEA and LCA studies are needed to assess their performance in point-source applications.

As previously discussed, ATS systems have the potential for nutrient remediation for point sources but have not been integrated with WWTP infrastructure. Currently, commercial

scale ATS systems are mostly used for surface water treatment, where they have been shown to reduce nutrient concentrations effectively, however, the biomass often goes unutilized [12]. Algal biomass holds significant potential as a feedstock for a variety of biofuels products, such as renewable diesel [13], [14], and can also be used to produce biochar–a carbon-rich material with carbon sequestration and soil amendment applications [15], [16]. Furthermore, algal biomass contains high-value biochemical compounds—such as antioxidants, omega-3 fatty acids, and polysaccharides—that are extracted for use in pharmaceutical and cosmetic applications due to their bioactive and therapeutic properties [17]. Therefore, ATS systems not only have the potential to contribute to water quality improvement but also to generate feedstock for commodities and high-value products, furthering the goals of sustainable water management and a circular bioeconomy.

In addition to nutrient removal, several studies have investigated the economic feasibility and environmental impacts of downstream algal biomass processing for biofuel production [9], [13], [14], [18], [19], [20], [21], [22]. Cruce et al. (2021) modeled biofuel production across various algal cultivation systems and reported costs ranging from \$0.42 to \$8.96 LGE^{-1}, with higher values attributed to photobioreactors and open raceway ponds (ORPs) due to their substantial capital expenditures (CAPEX) [21]. Notably, ATS systems were shown to require lower energy input and operational expenditures (OPEX) than traditional suspended algal systems, primarily as a result of more efficient biomass separation [21]. Greene et al. (2025) modeled renewable diesel production from ORP-grown biomass via hydrothermal liquefaction (HTL), with estimated fuel prices ranging from \$3.72 to \$7.26 LGE^{-1} [13]. In contrast, Banks et al. (2023) evaluated HTL conversion of biomass from ATS systems and reported a cost range of \$1.32 to \$6.61 LGE^{-1} [9]. When the value of water treatment services was incorporated, the

modeled fuel price was further reduced—reaching as low as −$9.25 LGE^{-1} in some case study locations—thereby achieving net profitability [9]. From a life cycle perspective, ATS-derived biofuels were also associated with lower global warming potential (GWP). While ORP-based biofuels exhibited a GWP between 28.9 and 65.9 g CO_2-eq MJ^{-1} [13], ATS-derived biofuels have been reported to achieve values as low as 25 g CO_2-eq MJ^{-1} [9]. Collectively, these studies indicated that ATS-based systems generally offered lower production costs and GWP compared to dedicated algal farms utilizing alternative cultivation architectures such as ORPs and photobioreactors.

Previous studies have shown that ATS systems provide both biomass production and nutrient removal, supporting the application of nutrient credits for their water treatment benefits–particularly through the removal of nitrogen and phosphorus from wastewater. Published studies have evaluated the impact of these nutrient credits on the costs of algal biomass for fuel applications [11], [23]. For example, Clippinger et al. (2021), explored the valorization of algal tertiary treatment in WWTP, considering a one-to-one equivalence for nitrogen and phosphorus removal, with a fixed price of \$4.5 kg^{-1} of nitrogen and phosphorus removed for bulk removal and \$67 kg^{-1} of nitrogen and phosphorus removed for dilute nutrient removal [24]. Contrastingly, Higgins et al. (2012) varied the values of nutrient credits between nitrogen (\$3.83 kg^{-1}) and phosphorus (\$9.57 kg^{-1}) [6]. One-to-one valuation does not account for the varying difficulty of removing nitrogen versus phosphorus. Phosphorus, for instance, is often more challenging to remove due to lower effluent concentration requirements and higher treatment costs [25], [26]. Therefore, differentiating the value of nitrogen and phosphorus removal is critical to enable a more accurate economic evaluation of nutrient removal from algal WWT.

While previous studies have explored the potential of ATS systems for nutrient removal and biofuel production, several key gaps remain. As discussed, published research has mostly focused on non-point-source pollution [9], [27] with limited exploration of point-source WWTP effluent. Deployment of ATS systems for WWTP effluent treatment requires exploring non-co-located systems, where algal cultivation (in WWTPs) and biofuel production (in centralized biorefineries) are geographically separated. Therefore, TEAs and LCAs of ATS systems integrated with WWTP must account for the costs and impacts of transporting biomass from treatment facilities to biorefineries to provide an accurate evaluation of the costs and environmental impacts of ATS-derived biofuels. Furthermore, existing TEA studies [9], [28], often rely on a simplified one-to-one equivalence for nitrogen and phosphorus nutrient credits, overlooking the differing removal efficiencies and costs associated with each nutrient.

To address key limitations in the existing literature, this study distinguishes itself by focusing on the deployment of ATS systems for point-source WWTP effluent treatment, considering non-co-located configurations for large-scale biomass-to-biofuel conversion, and introducing a differentiated framework for nutrient credit valuation for both nitrogen and phosphorus. This work integrates geographic nutrient loading data with process modeling, TEA, and LCA to evaluate the economic and environmental impacts of ATS systems for simultaneous water quality improvement and renewable diesel production across the continental United States (CONUS). The analysis offers a comprehensive assessment of technical feasibility and system performance under region-specific conditions, including nutrient loads, flowrates, and electricity grid. Results identify regions where ATS integration is economically viable, highlight primary cost drivers, and quantify environmental trade-offs associated with algal biofuel production. The discussion focuses on the research and development efforts needed to improve the cost

competitiveness of ATS-based fuel pathways and compares ATS performance with other tertiary treatment technologies. This work represents a significant contribution to advancing sustainable wastewater management practices and offers a promising pathway for decarbonizing the transportation sector through algae-based technologies.

2. METHODOLOGY

This study investigates the entire process of algae-based wastewater treatment through ATS systems and the subsequent conversion of harvested biomass into renewable diesel production via HTL. A modular process model was developed to evaluate the mass and energy flows of an ATS facility that treats WWTP effluent. Process model outputs informed the LCA and TEA to evaluate the economic feasibility and environmental impacts of algal biofuels from ATS derived biomass. The following sections detail the methods used for this analysis, including the process model (Section 2.1), TEA (Section 2.2), and LCA (Section 2.3).

2.1 Process Model

2.1.1 System Boundary

The system boundary used in this study included algae-based nutrient removal through ATS and biomass conversion to renewable diesel. The spatial boundary of the study was defined to include WWTPs across CONUS, where total nitrogen and total phosphorus load data were linked to Hydraulic Unit Code (HUC) 12 sub-watershed codes for geospatial analysis. The temporal boundary includes annual data from the 2022 EPA Nutrient Model [29] with the algae cultivation model operating year-round, except during freezing conditions. As illustrated in Figure 1, the system boundary was defined to include the full life cycle of the process. Nutrient removal and biomass production were carried out by ATS systems, followed by centralized downstream processing of the biomass, which included ash reduction, HTL, and fuel upgrading through hydrotreating and hydrocracking, as well as transportation of the produced fuel and its end use through combustion. The system boundary was defined to ensure a focused analysis on the algae-based nutrient removal process and renewable diesel production, while geographic

variability in wastewater flow and nutrient concentrations was addressed through the integration of plant-specific data.

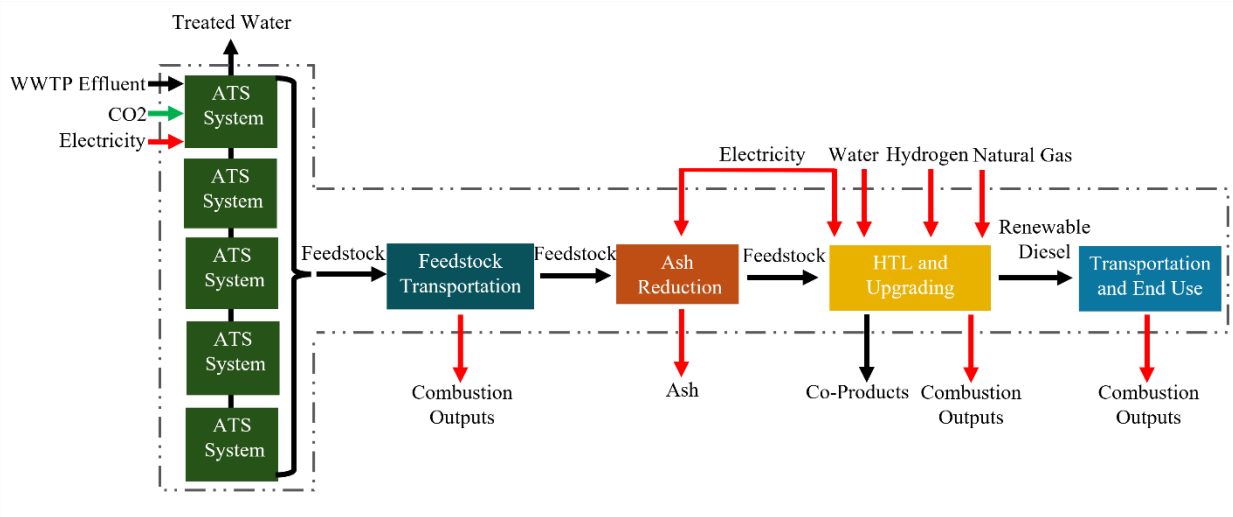

Figure 1. Process flow diagram of an algal turf scrubber (ATS) for treatment of wastewater treatment plant (WWTP) effluent and production of renewable diesel. Biomass harvested from each ATS is transported to a centralized biorefinery, where it undergoes pretreatment followed by conversion to renewable diesel through hydrothermal liquefaction (HTL), hydrotreating and hydrocracking.

2.1.2 Data Collection and Preprocessing

Flowrate, total nitrogen, and total phosphorus data were sourced from the 2022 Nutrient Model by the EPA (Hypoxia Task Force Search), which was made available through the Water Pollutant Loading Tool [29]. Total nitrogen and total phosphorus loading data were obtained from the EPA Nutrient Model, which provided estimated nutrient discharges for wastewater treatment facilities operated under current EPA National Pollutant Discharge Elimination System (NPDES) permits. Facility-level attributes such as total annual wastewater flow was included in the EPA nutrient dataset, along with HUC12 sub-watershed codes, which were used to enable geospatial analysis (Figure A2 and A3). The dataset was filtered and analyzed following the

methodology outlined by Limb et al. [26]. The nitrogen and phosphorus datasets were merged using NPDES permit numbers. Locations with missing total nitrogen or total phosphorus data were excluded from the analysis. Non-wastewater treatment plants were excluded based on Standard Industrial Classification codes, North American Industry Classification System codes, and facility name. Locations lacking these codes were retained if their titles indicated wastewater or sewage treatment. Missing HUC data were assigned by matching the latitude and longitude of each location to the respective HUC12 and HUC6 regions within the dataset.

Regional weather data was sourced from the Typical Meteorological Year (TMY3) dataset and subsequently processed and analyzed using the methods outlined by Banks et al. (2023) [9]. Annual global horizontal irradiance (GHI) data were mapped to each HUC8 subbasin following the approach described by Greene et al. (2021) and Beattie et al. (2021) [30], [31]. Operational days for each HUC8 subbasin were determined using the algal thermal algae pond model described by Quiroz et al. (2021) [32], under the assumption that the ATS system was functional on all days that did not experience freezing temperatures. Once each HUC8 subbasin was assigned an annual average GHI and operational days value, these data were paired to each WWTP by linking HUC12 locations to HUC8 regions based on latitudes and longitudes. A total of 12,455 WWTP locations were identified and included in the cultivation model for analysis.

2.1.3 Cultivation and Downstream Processing

Algal biomass cultivation was modeled at the HUC12 resolution, and the results were aggregated to HUC6 regions to generate regional-scale maps. A depiction of a HUC6 location is provided in Appendix A (Figure A1). The modeled cultivation system consisted of a holding tank and an ATS unit that operated in batch mode, where the system is loaded with the total volume of wastewater effluent and the total volume leaves the ATS after treating. To simplify the analysis,

the study excluded land availability constraints and did not implement a fractionated flow approach for recirculation. Results were then fed into the downstream processing model for HTL to generate TEA and LCA results on a HUC6 resolution. A schematic of the modeled ATS system is provided in Appendix A (Figure A6), and key model inputs are summarized in Table 1.

Productivities at each HUC12 WWTP were calculated following the methodology established by Banks et al. (2023), which incorporated TMY3 meteorological data and outdoor productivity data for an ATS system located in Laguna Madre, TX (25° N, 97° W) [33]. A dataset of 21 productivity measurements collected over a six-month field trial (January 2018 to June 2018) was employed to validate a first-order algal growth model [9]. The first order growth model used an average light efficiency of 2.8%, corresponding to a US maximum productivity of 25 g m^{-2} day^{-1} which is optimistic compared to pilot- scale deployments [9], [12], [33]. The productivity calculation (Equation A1) and modeled productivity values at each HUC6 watershed (Figure A5B) are provided in Appendix A.

Subsequently, productivity and biomass composition data were used to calculate nitrogen and phosphorus removal rates. Experimental biomass composition data were obtained from indoor cultivation trials using recirculating ATS systems. These systems were designed to replicate higher nutrient concentrations, typically observed in WWTP effluent, with influent nutrient levels maintained at 15 ppm total nitrogen and 5 ppm total phosphorus. A modified L1 media recipe (Table A1) was used, with nitrogen and phosphorus replenished twice weekly and complete media replacement performed once a month. Flow-ways were operated between December 2024 and March 2025 under continuous flow conditions of 2.07 L s^{-1} m^{-1} of channel width and harvested weekly. A constant water temperature of 23 °C was maintained using electric chillers, and pH was kept at 8 via CO_2 sparging. Each unit was also illuminated for 16

hours per day at a light intensity of 1000 μmol s^{-1}. Biomass compositional data obtained from this growth campaign are provided in Table 1.

Because nutrient loads and flow conditions varied across WWTPs, each ATS system was individually sized and optimized to meet EPA Level 5 effluent limits of 2 mg L^{-1} total nitrogen and 0.02 mg L^{-1} total phosphorus [2]. Decision variables included linear hydraulic flowrate (LHFR), length-to-width ratio (L:W), and recirculation cycles. Ranges for LHFR (2.07 – 8.28 L s^{-1} m^{-1}) and L:W (2– 4) were fixed based on previous ATS designs by HydroMentia [12]. Land availability was not considered in this study; therefore, the number of recirculation cycles was left unconstrained. Flow was recirculated as needed to achieve Level 5 nutrient removal targets, which resulted in larger system sizes. For scenarios requiring recirculation, the total flowrate treated by the ATS system was calculated by multiplying the WWTP effluent flow by the number of recirculation cycles. Since recirculating configurations require additional infrastructure, an influent holding tank and separate tanks for managing recirculated flow were modeled. Based on the optimized system parameters, the required ATS width was calculated by dividing the total flowrate by the LHFR, while the system length was determined using the specified L:W ratio. The total system area was then used to estimate annual biomass production and total nutrient removal. Electricity demand for the ATS was scaled according to system requirements, where the pumping power assumption is provided in Table 1, and the energy consumption calculation can be found in Appendix A (Equation A2).

Biomass output was calculated for each ATS system at the HUC12 resolution. For each HUC6 region, the geographic coordinates of the associated biorefinery were determined by averaging the latitude and longitude of all HUC12 locations within that region. Transportation distances were then calculated from this central biorefinery location to each ATS facility within

the corresponding HUC6. Total biomass transported, assumed at 20% solids, was computed as the sum of biomass from all ATS systems within the HUC6 basin. Transportation impacts were estimated using the average distance between ATS facilities and the central biorefinery.

Table 1. Inputs to cultivation and downstream processing models.

Parameter	**Value**	**Units**	**Reference**
Cultivation Model			
Target Total Nitrogen	2	mg L^{-1}	[2]
Target Total Phosphorus	0.02	mg L^{-1}	[2]
Total Nitrogen	HUC12-resolved (varied)	mg L^{-1}	[29]
Total Phosphorus	HUC12-resolved (varied)	mg L^{-1}	[29]
Flow Rate	HUC12-resolved (varied)	MGD	[29]
Operational Days	HUC12-resolved (varied)	days	[9]
Global Warming Potential	HUC12-resolved (varied)	W m^{-2} day^{-1}	[9]
Light Efficiency	2.8	%	[9]
Biomass Elemental Composition			
Ash	20	% of solids	Experimentally Validated

Carbon	50	% of ash free solids	Experimentally Validated
Nitrogen	10	% of ash free solids	Experimentally Validated
Phosphorus	1	% of ash free solids	Experimentally Validated
Nitrogen to Phosphorus Molar Ratio	22		Experimentally Validated
ATS Design Variables			
Linear Hydraulic Flowrate	2.07 – 8.28	$L\ s^{-1}\ m^{-1}$	[12]
Length to Width Ratio	2 – 4		[12]
Pump Energy Use	0.096	$kWh\ m^{-3}$	[12]
Other Energy Use	10	% of pump energy	[12]

2.1.4 HTL Model

The HTL model followed the work of Chen et al. (2021), with ash reduction methods from Banks et al. (2023) [9], [19]. The biomass goes through pretreatment to reduce the ash content to 12 wt%, followed by HTL conversion, which yields biocrude, aqueous organics, gaseous products, and biochar. The biocrude is subsequently upgraded into diesel, naphtha, and heavy oil fractions. The heavy oil is further hydrocracked to increase the diesel and naphtha yield. Yields of biocrude, aqueous phase, gas, and biochar were determined based on the fixed biomass composition of the feedstock, which was applied uniformly across all WWTP scenarios.

The feedstock solids were assumed to contain 5% lipids, 52% proteins, 31% carbohydrates, and 12% ash by weight, based on DeRose et al. (2019) [20]. Additional model parameters for the HTL system are summarized in Appendix A (Table A2).

2.2 Techno-Economic Analysis

TEA is a systematic method used to evaluate the economic viability of a technology by integrating process model data with costing models. This approach estimates the financial performance of a system, including factors such as capital and operating costs, revenue generation, depreciation, and return on investment. Cost assumptions for the systems included detailed cost breakdowns for equipment, labor, and OPEX. Equipment costs were indexed to the year 2024 using the corresponding Chemical Engineering Plant Costs Index [34]. Chemical costs were indexed using Producer Price Index by Commodity [35]. Finally, labor costs were indexed to 2024 using Current Employment Statistics [36]. Accordingly, all TEA results are reported in 2024 U.S. dollars.

For this study, an individual TEA was applied to the ATS and HTL processes. The cost assumptions for the ATS system were sourced from DeRose et al. (2021) and are summarized in Appendix A (Table A4) [10]. The assumptions include capital and operational costs for land acquisition, infrastructure, growth systems, and harvesting. Land costs were modeled using average prices for marginal land suitable for non-food, non-residential development, based on county-level USDA datasets [37]. Costs for recirculation tanks were based on total volume requirements, with costs scaled using industry-standard tank cost curves reported by the EPA [38]. The growth system and harvest equipment costs were retrieved from DeRose et al. (2021) and represent an average of different ATS water treatment TEAs [10].

Downstream processing costs were estimated following the methodology established by Chen and Quinn [19], with updated cost parameters for the hot oil heat exchanger, knockout drum unit, and labor [19], [39]. The average feedstock cost aggregated at the HUC6 resolution was used to represent the delivered cost of biomass entering the biorefinery. A feedstock transportation cost of \$ 0.036 km^1 m^{-3} feedstock [40] was used to estimate the total feedstock transportation costs. De-ashing costs were implemented using data from a water wash ash-reduction system [10], [41]. Co-products included fertilizers from ammonia and diammonium phosphate (DAP) at a fixed cost of 0.45 and 0.37 \$ kg^{-1}, respectively. Additional cost breakdowns and economic assumptions used in the TEA can be found in Table A5 in the Appendix A.

A discounted cash flow rate of return (DCFROR) analysis was used to calculate the minimum biomass selling price (MBSP) for biomass produced by the ATS system, assuming a net present value of zero. Financial parameters were based on the "Nth-of-a-kind plant" assumptions presented by the U.S. Department of Energy's Bioenergy Technologies Office (BETO) and are listed in Table A3 in Appendix A [42]. BETO provides standardized techno-economic modeling guidelines for mature commercial-scale systems, including values for internal rate of return, loan interest rate, and a 7-year modified accelerated cost recovery system depreciation scheme [42]. Similarly, TEA was conducted for each HUC6 subbasin across CONUS to estimate the minimum fuel selling price (MFSP) of renewable diesel produced via HTL.

Furthermore, nutrient credits were incorporated into the TEA to evaluate the economic impacts of nutrient removal by ATS systems, considering their potential to generate additional revenue through providing a water treatment service. The nutrient credit values were based on

the conventional treatment costs for EPA Level 5 gray infrastructure treatment, as determined by Limb et al. [26]. Specifically, total nitrogen was priced at \$42 kg^{-1} and total phosphorus was priced at \$321 kg^{-1}, representing the costs of membrane bioreactors (MBR) with sidestream reverse osmosis (RO) technology [26]. For Level 4 credits, total nitrogen was priced at \$20 kg^{-1} and total phosphorus was priced at \$225 kg^{-1}, representing the costs of a 4 Stage Bardenpho Membrane Bioreactor [26].

2.3 Life Cycle Assessment

LCA is a comprehensive methodology used to evaluate the environmental impacts associated with a product or process across its entire life cycle—from raw material extraction through production, use, and end-of-life disposal or recycling. An attributional LCA was applied to assess the environmental impacts of renewable diesel produced via ATS. A well-to-wheels system boundary, that covered biomass cultivation, fuel production, and end-use phases, was employed. Infrastructure-related emissions were excluded from the analysis, as the assumed plant lifetime of 30 years renders their contribution negligible when averaged over time. Emissions associated with feedstock transportation were included in the analysis to capture the impact of non-co-located ATS and biorefinery facilities. The functional unit for the LCA was defined as the production and use of 1 megajoule (MJ) of total fuel, including both naphtha and renewable diesel.

In addition, wastewater treatment credits were not included, as the ATS system was modeled as a supplementary unit to existing WWTP infrastructure. This approach aligns with an attributional LCA framework, treating the system as a potential future addition implemented in response to stricter nutrient discharge regulations, rather than a full replacement of existing treatment technologies. Co-product credits from recovered nutrients in the aqueous phase of HTL

were applied for fertilizer displacement, accounting for avoided emissions associated with the production of conventional synthetic fertilizers (e.g. nitrogen and diammonium phosphate). A credit for carbon sequestration was also included to reflect the storage potential of biochar generated during the HTL process.

Life cycle inventory (LCI) data were sourced from the Ecoinvent Version 3.4 database [43]. The TRACI 2.1 assessment method was used to evaluate ten impact categories: GWP, acidification, ecotoxicity, human health (carcinogenic and non-carcinogenic), ozone depletion, photochemical ozone formation, fossil fuel depletion, and respiratory effects [44]. GWP values of 1, 29.8, and 273 for a 100-year time horizon for carbon dioxide, methane, and nitrous oxide respectively, were used based on values reported in the IPCC 6th Assessment Report [45]. Electricity impacts were modeled at a North American Electric Reliability Corporation resolution. Freight lorry transport was used to model feedstock delivery, based on Ecoinvent LCI data.

3. RESULTS AND DISCUSSION

The following section presents results from the TEA and LCA of ATS systems for the provided nutrient reduction and renewable diesel production scenarios. TEA and LCA were conducted for the full system at each HUC6 location, generating results across the CONUS. Maps are provided to illustrate the spatial variation in economic feasibility and GWP of algal-based renewable diesel. Additionally, MFSP and GWP breakdowns are presented for select case study HUC6 basins—Upper Hudson, Little Colorado, and South Florida—to explore regional trends. Together, these results offer insights into the national-scale economic and environmental implications of deploying ATS systems for wastewater treatment and renewable fuel production.

3.1 Techno-Economic Analysis

Results at a HUC6 watershed level are shown in Section 3.1.1 to address trends at a regional scale and present locations economically feasible for fuel production with ATS systems deployed at the end of WWTPs. Section 3.1.2 presents case study locations that highlight the main drivers of MFSP. Results highlight the influence of nutrient credits on economic feasibility of fuel production with ATS to HTL pathway and illustrate trade-offs between operational and capital expenditures.

3.1.1 Watershed-Level Techno-Economic Analysis Results

Geographically resolved results, illustrated in Figure 2A, demonstrate that ATS-derived algal biofuel is generally not economically viable without nutrient credits. The calculated MFSP ranged from \$5.29 LGE^{1} to \$202 LGE^{-1}, with a few outliers exceeding \$300 LGE^{-1} (Figure A10). Key factors influencing MFSP include algal productivity, length of the operational season,

and influent nutrient loading. Lower MFSP values (ranging from \$5.29 to \$13.23 LGE^{-1}) were observed in the southwestern U.S., primarily driven by high productivity (> 20 g m^{-2} d^{-1}) and extended operational days (Figure A5). Similarly, regions in the Pacific Northwest show relatively favorable MFSP, despite low productivity, due to longer operational days enabled by milder climates. For instance, the operational days in the northwest varied from 340 to 365 per year, compared to the lower operational days (220 – 240) observed in the Midwest (Figure A5A). However, productivity and operational days are not the only factors impacting MFSP, as nutrient loading was found to have a strong impact on costs (Figure A4). The economic performance of ATS systems was found to be influenced by nutrient loading, as system sizing is directly based on nutrient treatment capacity (Figure A7-S8). High nutrient loading in regions with limited productivity or short operational periods led to higher MFSP due to higher capital and operational costs. Conversely, even in areas with high productivity and extended operational windows (e.g. southwestern states), low nutrient concentrations may result in underutilized systems and similarly elevated MFSP. Thus, optimal economic performance depends on the balance between productivity, operational days, and nutrient loading.

As seen in Figure 2A, ATS systems without nutrient credits produce fuel that is not cost-competitive with the average gasoline fuel price of \$0.87 LGE^{-1} in 2024 [46], primarily due to high CAPEX and OPEX combined with limited fuel yield across all locations. However, when nutrient credits are applied, based on achieving EPA Level 5 nutrient reduction targets, 75% of locations yield MFSPs below \$0.87 LGE^{-1}. Furthermore, results in Figure 2B indicate that 57% of the total modeled HUC6 basins achieve an MFSP below -\$8 LGE^{-1}, resulting in a net economic return. These results demonstrate that nutrient credits are crucial for the economic

feasibility of ATS-based biofuel systems, where Level 5 treatment could generate a profit from fuel sales.

In addition, the results presented in Figure 2B indicate that nutrient loading, productivity, and operational days are key drivers of ATS system viability. In general, higher nutrient loadings reduce MFSP by increasing biomass production, thereby enhancing fuel yields and generating greater nutrient credit value. However, in locations with high nutrient loads, the increased costs of larger system infrastructure and operation can, in some cases, outweigh the benefits of additional biomass production and nutrient credits. For example, ATS systems deployed in South Florida exhibit elevated MFSPs ($9 LGE^{-1}), as the high operational and capital costs exceed the economic value of the nutrient credits. Conversely, basins with relatively low nutrient loadings can still achieve competitive MFSPs when paired with high productivity and extended operational days. In the Southwest, for instance, locations with low nutrient loads but high areal productivity demonstrate MFSPs between -$8 and $0 LGE^{-1}, when nutrient credits are applied. In these cases, the efficiency of nutrient removal and biomass utilization allows the nutrient credit to offset the cost of fuel production. A similar trend is observed in the Pacific Northwest, where MFSP values as low as –$8 LGE^{-1} were achieved despite low nutrient loading, driven by extended operational seasons with low freezing events. These patterns emphasize the importance of optimizing productivity and leveraging nutrient credits to make ATS-based biofuels more economically feasible.

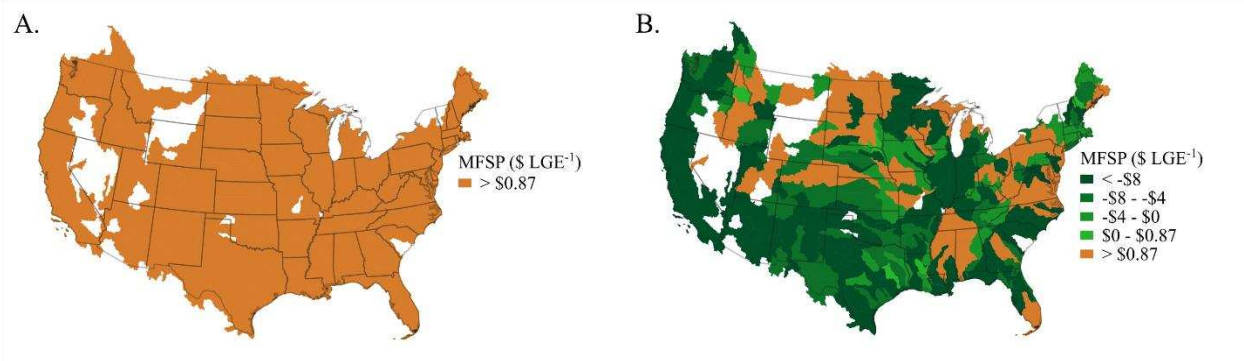

Figure 2. A) Minimum fuel selling price (MFSP) across the continental United States (CONUS), expressed in dollars per liter gasoline equivalent (LGE). B) MFSP across CONUS considering nutrient credits calculated for the Level 5 treatment scenario ($42 kg^{-1} for nitrogen and $321 kg^{-1} for phosphorus). White areas in both maps represent regions with missing nutrient data or zero wastewater flow.

3.1.2 Minimum Fuel Selling Price Breakdown

The breakdown of the MFSP for selected HUC6 basins, Upper Hudson, Little Colorado, and South Florida, reveals important insights into the cost structure of deploying ATS systems at different locations. As seen in Figure 3, for all locations, the majority of the MFSP is attributed to the cultivation process. However, the specific contributions of CAPEX of the cultivation stage varied significantly across basins, attributed to differences in the system scale required to achieve EPA Level 5 reduction targets. For example, Upper Hudson, which includes 101 facilities and a cumulative ATS facility area of 11000 hectares, presented the highest MFSP ($16 LGE^{-1}). This large area requirement was driven by the presence of multiple ATS systems treating high nutrient loadings at a low productivity (15 g m^{-2} day^{-1}). As a result, CAPEX contributed to 72% of the MFSP, highlighting the high infrastructure costs associated with system scaling in this watershed. South Florida, with 20 facilities and a cumulative area of 5750 hectares, exhibits a MFSP (16 LGE^{-1}) between those of Upper Hudson and Little Colorado. Like Upper Hudson, CAPEX is the largest contributor to MFSP at 62% due to high nutrient loadings requiring a larger area. In

contrast, Little Colorado, with only 8 deployed ATS facilities and a much smaller cumulative area of 0.045 hectares, presented the lowest MFSP ($14 LGE^{-1}) among case study locations. This is explained by the higher productivity (21 g m^{-2} d^{-1}) and low nutrient loads observed in Little Colorado basin. Results indicate that cultivation expenses–along with site-specific factors such as productivity and nutrient loading have a strong influence on ATS deployment costs across watersheds.

Moreover, building on these regional cost comparisons, the specific contributions of other processes in the system further illuminate the MFSP dynamics of ATS deployment across watershed basins. For example, the Little Colorado basin required a smaller cultivation footprint and produced less biomass compared to Upper Hudson and South Florida. As a result, transportation, along with the CAPEX and OPEX of downstream processing, contributed a larger share of the MFSP than cultivation CAPEX. Moreover, the electricity intensity (EI) of the Little Colorado ATS facilities is larger than Upper Hudson and South Florida, calculated as 2.6, 0.13, and 0.21 kWh kg^{-1} algae respectively. These differences in EI are primarily attributed to facility size and cycles required (Figure A8). Therefore, electricity costs, the main source of OPEX, were identified as a more prominent cost driver in Little Colorado and accounted for 71% of the MFSP, compared to 19% in Upper Hudson and 30% in South Florida. These findings highlight how regional variation in electricity use can shift the primary cost contributors and ultimately influence the cost drivers of ATS-based renewable fuel production.

However, for all locations, none of them were found to be economically feasible without considering nutrient credits. When nutrient credits are applied, the results presented in Figure 3 yield a significant reduction in MFSP across case study watersheds. In regions with high nutrient loadings, such as the Upper Hudson watershed basin, the net MFSP decreased by 78% from $16

LGE^{-1} to \$3 LGE^{-1}, due to the application of Level 4 nutrient credits. However, despite this reduction, the MFSP of Upper Hudson remained above the average costs of conventional fuel. In contrast, the Little Colorado basin experienced a 117% reduction, with MFSP decreasing from \$14 LGE^{-1} to -\$2 LGE^{-1}, making it economically favorable under the same crediting scenario. This is explained by the lower nutrient loadings (92 kg nitrogen day^{-1} and 17 kg phosphorus day^{-1}) and higher productivity (21 g m^{-2} day^{-1}) in Little Colorado compared to Upper Hudson which results in a larger nutrient credit. Furthermore, results highlight a trade-off between nutrient loadings and system productivity that affects economic feasibility. For instance, Upper Hudson has the lowest productivity (15 g m^{-2} d^{-1}) out of the case study locations but a higher nutrient loading (346 kg nitrogen day^{-1} and 46 kg phosphorus day^{-1}), leading to a high nutrient credit contribution to MFSP. On the other hand, Little Colorado has the highest productivity and the lowest nutrient loadings out of the three case study locations, but a larger nutrient credit contribution, which leads to the largest reduction in MFSP when Level 4 nutrients are considered.

Although South Florida has high nutrient loadings (1820 kg nitrogen day^{-1} and 162 kg phosphorus day^{-1}) and relatively high productivity (18 g m^{-2} day^{-1}), the impact of nutrient credit on MFSP is much lower compared to Upper Hudson and Little Colorado, with only a 29% reduction from \$16 LGE^{-1} to \$11 LGE^{-1} under Level 4 credit. South Florida has high nutrient loadings that require a higher ATS CAPEX and OPEX, whereas Upper Hudson, the nutrient credit does not outweigh ATS expenses. The average nutrient loading for total nitrogen in South Florida is 1820 kg day^{-1} which is far greater than the loading of 346 kg day^{-1} in Upper Hudson. Moreover, the nutrient loading in South Florida exceeds the threshold where returns are economically beneficial, which is why there is only a small reduction in MFSP. Overall, whether

the system has low or high productivity, nutrient credits contribute significantly to lowering MFSP.

As results indicate, nutrient credits play a critical role in achieving economic viability for fuel production from ATS systems. As the value of the nutrient credit increases, MFSP decreases accordingly, expanding the number of locations where ATS deployment becomes cost-effective (Figure A11). Under Level 5 nutrient credit scenarios, both Upper Hudson and Little Colorado achieve negative MFSPs of -$2 LGE^{-1} and –$11 LGE^{-1}, respectively, indicating profitable fuel production. Notably, Upper Hudson was not economically feasible at Level 4, highlighting the pivotal influence of higher credit levels in enabling feasibility. The transition from Level 4 to Level 5 nutrient credits results in MFSP reductions across all case study locations: a 47% decrease for Upper Hudson, 78% for Little Colorado, and 20% for South Florida. The pronounced MFSP reduction in Little Colorado is primarily due to the greater influence of phosphorus removal on the total nutrient credit. As previously described (Section 2.3), phosphorus removal is assigned to a higher economic value than nitrogen. Since phosphorus holds more weight in MFSP for Little Colorado, it benefits more substantially from increased nutrient credit levels. These findings underscore the importance of nutrient credit valuation in driving the economic feasibility of ATS-based biofuel production.

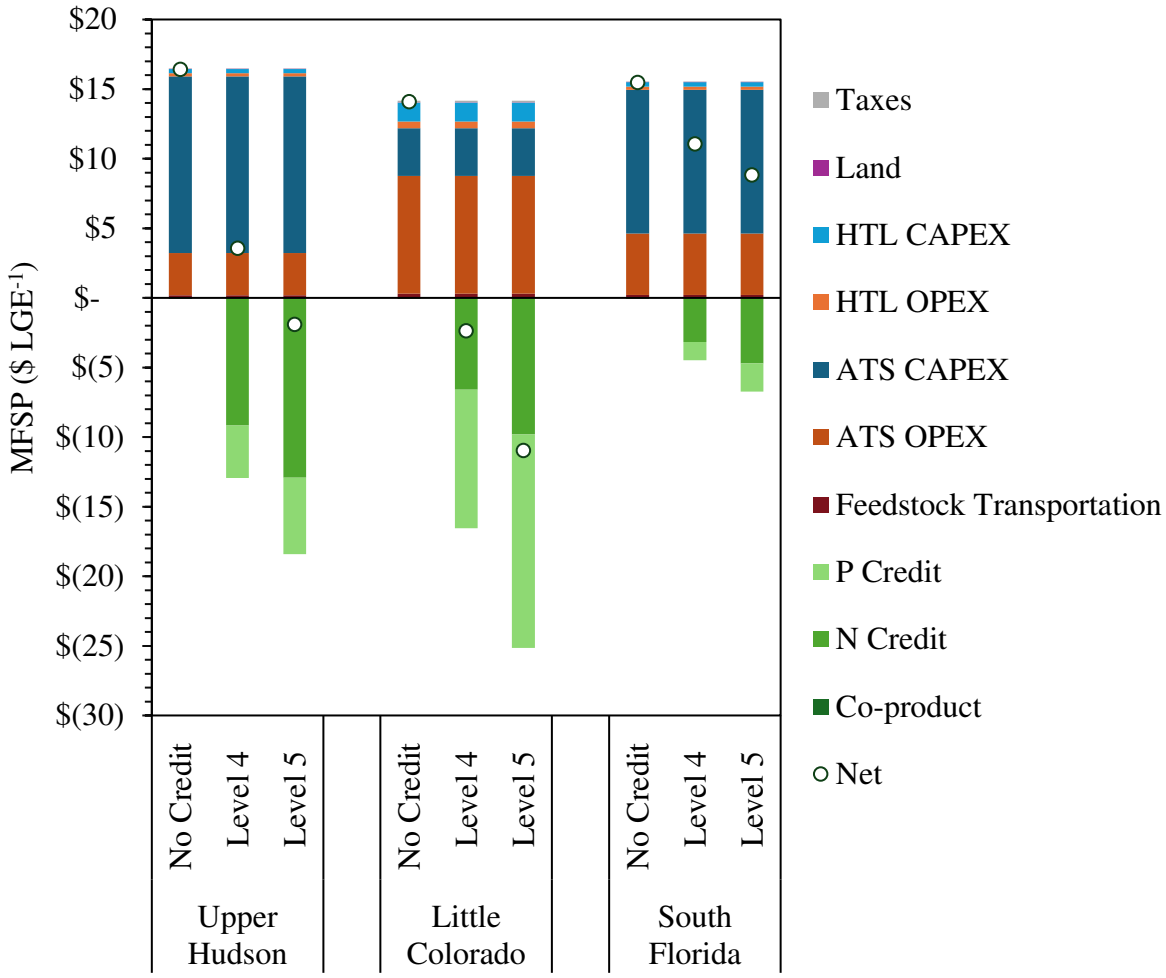

Figure 3. Minimum fuel selling price (MFSP) breakdown for three case study Hydraulic Unit Code 6 basins across three credit scenarios: without credits, with a credit calculated for Level 4 treatment ($30 kg^{-1} for nitrogen and $225 kg^{-1} for phosphorus), and a credit calculated for Level 5 treatment ($42 kg^{-1} for nitrogen and $321 kg^{-1} for phosphorus). The MFSP breakdown includes taxes, land cost, capital expenses (CAPEX), operational expenses (OPEX), and co-product revenue of fuel production via hydrothermal liquefaction (HTL) and CAPEX, OPEX, nitrogen removal credit (N Credit), and phosphorus removal credit (P Credit) from the Algal Turf Scrubber (ATS) systems.

3.2 Life Cycle Assessment

This section presents LCA results at a HUC6 watershed level (Section 3.2.1), illustrating the geographical variation of net GWP and ATS EI. A breakdown of case study watershed basins is provided in Section 3.2.2, to understand the drivers of net GWP. Furthermore, the net GWP

was compared to the Renewable Fuel Standard (RFS) of 45 g CO_2e MJ^{-1} to contextualize results [47]. This comparison is crucial for determining whether the environmental impacts of the system fall within regulatory limits for renewable fuel production.

3.2.1 Watershed Level Life Cycle Assessment Results

GWP results across CONUS, presented in Figure 4A, indicate that only a limited number of locations meet the Renewable Fuel Standard (RFS) threshold. In total, 68% of watershed basins exceed this GWP limit of 45 g CO_2e MJ^{-1}. Regions with higher nutrient loadings generally exhibited lower GWP values due to increased system scale, which supports greater biomass production and, consequently, higher fuel output. This results in improved energy efficiency and reduced emissions per unit of energy produced. In contrast, systems treating lower nutrient loadings are more energy-intensive; although they require smaller treatment areas, they still incur fixed energy demands while producing limited biomass, leading to elevated GWP values. The carbon intensity (CI) of regional electricity grids also influences GWP. For example, western CONUS regions, with an average grid CI of 0.389 kg CO_2e kWh^{-1}, showed lower GWP compared to Midwest regions with similar nutrient loadings but higher grid CI values (0.513 kg CO_2e kWh^{-1}) [43]. Despite this variation, nutrient loading remains the dominant factor influencing GWP. Locations with higher nutrient concentrations generally achieved lower EI and lower GWP, primarily due to the proportional relationship between nutrient removal and biomass production.

In addition, EI of downstream processing scales with the feedstock received, while the EI of the ATS facilities varied based on facility size and cycles required to treat influent nutrient loads. Therefore, GWP is strongly impacted by the EI of ATS systems. Figure 4B shows that GWP is correlated with the EI of ATS systems, confirming that electricity consumption is the

primary driver of lifecycle greenhouse gas emissions. Sites with high EI often correspond to systems with low nutrient loadings and low productivity, where energy input for pumping is high relative to the loading of nutrients treated and biomass produced. As nutrient loading decreases, EI tends to increase due to a tradeoff between energy use for pumping and biomass output. Moreover, ATS systems requiring higher recirculation rates exhibited elevated EI due to increased pumping demands. In contrast, larger systems may consume more absolute energy but distribute it more efficiently across greater biomass yields. For instance, South Florida exhibits high nutrient loadings, large facility area (Figure A8A), but a lower cycle requirement (Figure A8B) allowing the location to achieve low EI (0.21 kWh kg^{-1} algae) and a low GWP (25 CO_2e MJ^{-1}). When compared to traditional algal cultivation in open raceway ponds, ATS systems in this study were found to be less energy intensive. Specifically, 60% of ATS facilities exceeded the 1.4 kWh kg^{-1} algae EI benchmark reported for cultivation in open pond systems for fuel applications [21]. While ATS has been cited in literature as having lower EI than raceway ponds, this study shows the opposite trend, largely due to the high energy demands of cyclic treatment processes required for nutrient removal from point-source wastewater effluent. Therefore, improvements in ATS system design are necessary to reduce energy intensity in the cultivation stage.

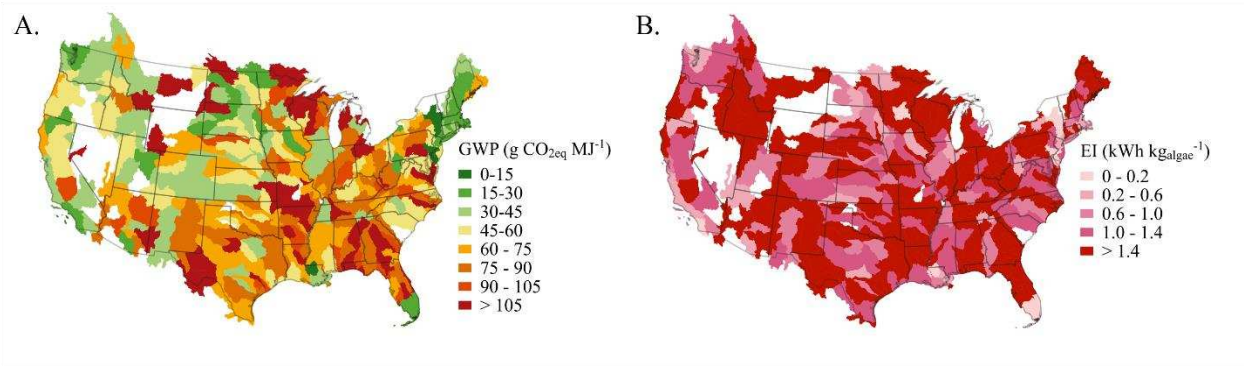

Figure 4. A) Net global warming potential (GWP) across the continental United States (CONUS) for each Hydrological Unit Code 6 (HUC6) basin. Locations in green meet the Renewable Fuel Standard (45 g CO_2e MJ^{-1}). B) Electricity intensity of Algal Turf Scrubber systems aggregated to a HUC6 basin level across CONUS, expressed in kilowatt-hours per kilogram of ash free dry biomass produced (kWh kg_{algae}^{-1}). White areas in both maps represent regions with missing nutrient data or zero wastewater flow. A visual of these maps in different colors is presented in Appendix A (Figure A12).

3.2.2 Global Warming Potential Breakdown

The breakdown of GWP for selected HUC6 basins, Upper Hudson, Little Colorado, and South Florida, provides insights into the specific drivers of greenhouse gas emissions for ATS systems deployed across different regions. As shown in Figure 5, the lifecycle GWP of algal-based biofuel produced in both Upper Hudson (12 g CO_2e MJ^{-1}) and South Florida (25 g CO_2e MJ^{-1}) meet the RFS, while Little Colorado (97 g CO_2e MJ^{-1}) exceeds it. The lower GWP observed in Upper Hudson and South Florida is primarily attributed to more efficient electricity use in their ATS systems compared to Little Colorado. The differences in GWP across locations emphasize how location-specific factors, such as EI, affect the GWP of ATS systems.

The GWP contributions from various stages of the ATS process are compared in Figure 6. As expected, the contribution from conversion is similar across all three regions due to a fixed biomass composition, with these stages being primarily responsible for the CO_2 emissions associated with downstream processing. In contrast, the transportation stage, which accounts for

the GWP from transporting biomass to the biorefinery, varied across locations. For Little Colorado and South Florida, transportation contributes a larger portion to GWP, as these regions have fewer facilities compared to Upper Hudson. As a result, biomass must be transported over longer distances, increasing the GWP contribution from this stage. The cultivation stage, while not the largest contributor to GWP in some locations, is the most variable across locations, with values of 1.5, 75, and 7.7 $CO_2e\ MJ^{-1}$ for Upper Hudson, Little Colorado, and South Florida, respectively. This variability in impact of cultivation on GWP is primarily due to differences in electricity use across regions, as previously discussed. As the EI of cultivation fluctuates due to differences in size of the system and cycles required, it significantly influences GWP, explaining the variations observed between case study regions.

In addition to the direct GWP contributions, co-product credits from displacement of conventional emissions provide minor offsets. Specifically, ammonia and diammonium phosphate (DAP) credits reflect the displacement of GHG emissions associated with conventional fertilizer production. As shown in Figure 5, ammonia offers a greater contribution to GWP reduction compared to DAP due to its higher displacement potential. Moreover, Figure 5 illustrates the carbon balance across the system, including CO_2 uptake during algal growth, CO_2 emissions from the aqueous and gas phases during conversion, and CO_2 released during end-use combustion. The fraction of carbon not emitted during these stages is retained in the biochar, contributing a small GWP credit through long-term carbon sequestration. This negative biochar credit reflects the storage of carbon in HTL-derived biochar, which remains stored rather than emitted to the atmosphere. However, the overall impact of these displacement and carbon sequestration credits is minimal and does not substantially reduce the total GWP of the system, suggesting that process-level improvements—such as reducing energy use during cultivation and

material inputs in conversion—offer a more effective pathway for achieving meaningful GWP reductions.

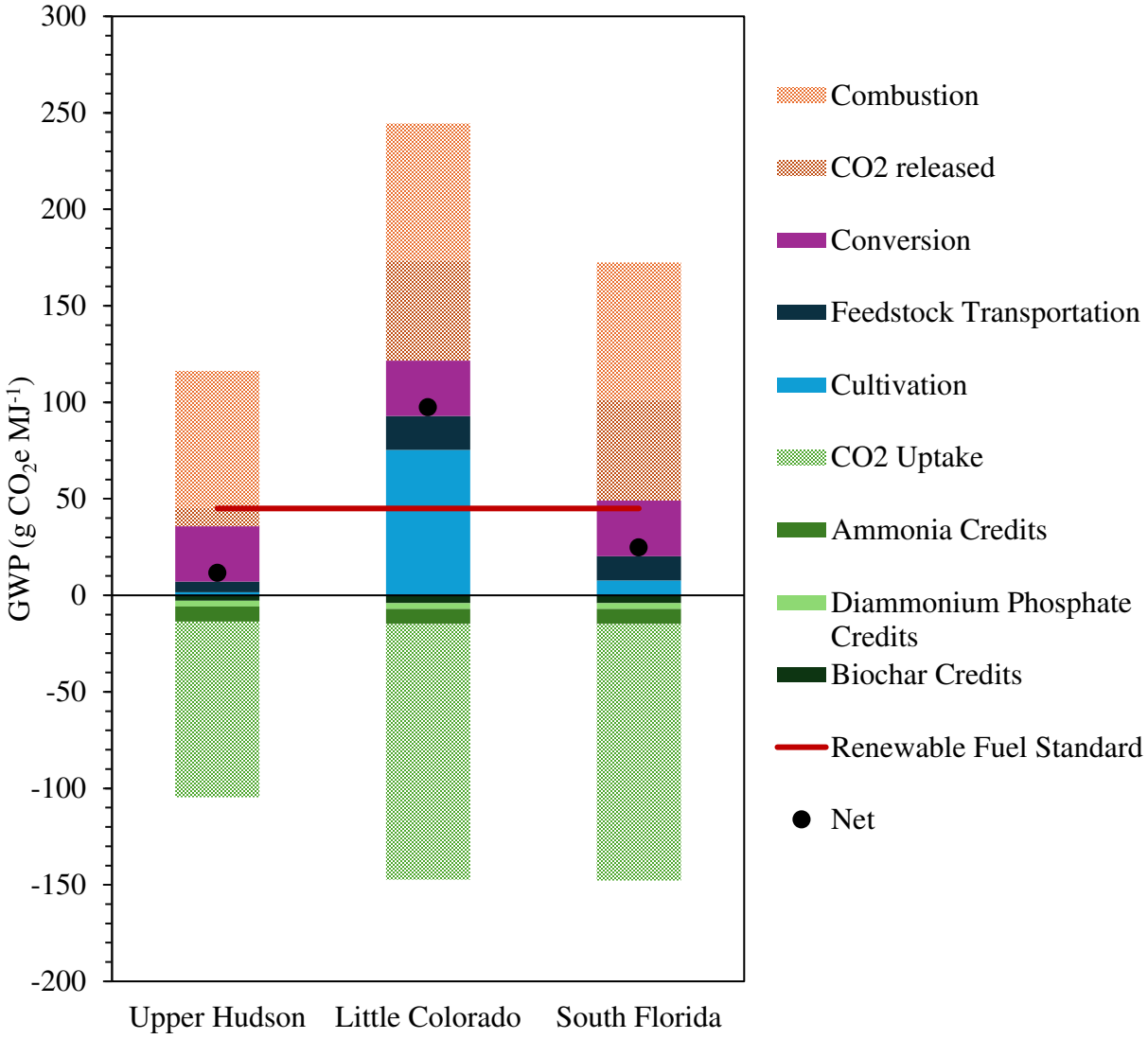

Figure 5. Breakdown of global warming potential (GWP) for three case study Hydraulic Unit Code 6 basins. The GWP includes emissions from cultivation, transportation, conversion, CO_2 released from aqueous and gas phases in hydrothermal liquefaction, and combustion, as well as credits from CO_2 uptake by biomass, displacement of fertilizer production (ammonia and diammonium phosphate (DAP)), and carbon sequestration via biochar. Renewable Fuel Standard is marked by a red line.

3.3 Implications

This study highlights the critical role of nutrient credits to make fuel production with ATS systems economically viable. However, beyond biofuel generation, ATS systems can also be evaluated based on their nutrient removal performance, offering a compelling alternative to conventional WWTP technologies. When evaluated solely as a treatment technology, nearly all modeled ATS systems demonstrated superior performance relative to conventional gray infrastructure. For example, only 2% of ATS systems exceeded the GWP benchmark of 1.2 kg CO_{2eq} m^{-3} associated with Level 5 gray treatment technologies, such as membrane bioreactors (MBR) with sidestream reverse osmosis (RO) [26]. Furthermore, approximately 99% of ATS systems operated below the benchmark cost of \$1.61 m^{-3} (in 2022 dollars) defined for MBR + RO systems, highlighting their potential for cost-effective, low-carbon nutrient management [26].

In cases where nutrient removal is the focus, the biomass generated becomes a co-product rather than the main output, with a range of potential applications depending on its composition and prevailing market conditions. Biomass produced from ATS systems may be used in lower-value applications such as land-applied fertilizers or soil amendments (e.g., biochar), which can displace synthetic fertilizer use and contribute to carbon sequestration [16]. Alternatively, higher-value applications, such as the extraction of bioactive compounds, pigments (e.g., phycocyanin), or precursors for bioplastics and pharmaceuticals could substantially improve the economic viability of ATS systems, particularly when integrated into a biorefinery model [17], [48]. The suitability of these applications depends on biomass composition, including lipid, protein, and carbohydrate content, as well as the presence of contaminants that may limit end-use markets. Therefore, selecting the optimal biomass utilization pathway requires alignment with regional

market demands, regulatory frameworks, and the specific biochemical profile of the produced algae.

Moreover, the results presented in this study demonstrate the biomass productivity potential of integrating ATS into tertiary treatment processes within WWTPs. However, the feasibility of ATS systems must consider the scale of achievable renewable fuel production. For instance, only a limited number of locations are capable of producing more than 40 MLGE yr^{-1} (Figure A9), suggesting that ATS systems at WWTPs typically contribute only a modest quantity of renewable fuel. This study emphasizes that the relatively low biomass output from ATS systems is primarily a result of the scale of the facilities, driven by flow rates and nutrient concentrations. To improve biofuel production, future research efforts could focus on integrating secondary treatment sludge from WWTPs into the feedstock for biorefineries, as this sludge is rich in organic matter [49]. Furthermore, the increased deployment of ATS systems for both point-source and non-point-source wastewater treatment could bolster feedstock availability, thereby improving fuel production in centralized biorefineries. Non-point-source systems, which typically utilize larger-scale ATS configurations than those studied here, could be integrated with point-source treatment systems to combine biomass from both sources [9]. This combined biomass could then be transported to biorefineries, facilitating an increase in renewable fuel production. Through enhancing fuel production by exploring various avenues, ATS fuel production would contribute more substantially to the decarbonization of heavy-duty transportation.

Advancements in ATS system design represent another critical opportunity for enhancing overall productivity and process efficiency. Yields in this study represent optimistic values based on a maximum productivity of 25 g m^{-2} day^{-1}. While the current model accounts for light

intensity, it does not incorporate temperature effects in the productivity calculation, despite the temperature being a well-established driver of algal growth kinetics [50]. Future improvements could include integrating algae growth models that consider both light and temperature to better capture the dynamics of biomass production. Optimized productivity is important for maximizing biomass yields and minimizing operational costs. This can be achieved by refining system parameters such as harvest frequency, light distribution, nutrient delivery, and surface area utilization, all of which influence algal growth kinetics [51], [52], [53]. In addition to system design, improving the lipid content of algal biomass remains a key target for increasing fuel yield and achieving economic viability [54]. Lipid-rich strains or cultivation conditions that favor lipid accumulation could shift the value proposition of ATS systems toward more profitable fuel pathways, including sustainable aviation fuel. However, this requires careful balance with nutrient removal goals and overall biomass productivity. Together, these innovations in system design and biomass optimization are essential for maximizing the multifunctional benefits of ATS systems and advancing their role in integrated water-energy nexus solutions.

While ATS systems have shown strong nutrient removal capabilities, consistent achievement of low phosphorus concentrations (e.g., ≤ 0.02 mg L^{-1}) has not yet been validated at scale, particularly under single-pass configurations [55]. Integration of recirculation may help achieve such performance but requires further investigation under real-world conditions. As the current model assumes batch operation, large-scale deployment would benefit from dynamic flow configurations such as continuous or fractionated flow systems. These strategies can prevent carbon limitation, a common constraint in recirculating systems, by maintaining consistent inorganic carbon availability [56]. Methods such as flow partitioning between the ATS and a reservoir, or bicarbonate supplementation, may be effective in sustaining the effective

nutrient removal presented in this analysis. Future work should also assess land availability constraints, particularly in densely developed or geographically limited regions, which may affect system scalability. Additionally, transportation logistics for non-co-located ATS and biorefinery configurations must be further investigated, as biomass hauling distances and methods can significantly influence both GWP and MFSP outcomes. Improved assumptions for flow management and spatial deployment will be critical for realizing the full potential of ATS systems as multifunctional platforms for water treatment and biofuel production.

4. CONCLUSIONS

This study provides the first combined TEA and LCA of ATS systems applied to point-source WWTPs, offering a comprehensive and data-driven assessment of their dual role in nutrient removal and biofuel production. By integrating detailed process modeling with region-specific nutrient data, this work establishes a robust foundation for evaluating the environmental and economic performance of ATS systems at scale. A key contribution of this study is the use of differentiated nutrient credits for nitrogen and phosphorus, which provide a more accurate and realistic valuation of nutrient removal services. By accounting for operational separation and biomass transport logistics – often overlooked in previous studies – this work provides critical insight into the practical challenges and opportunities for real-world implementation of ATS systems. The results demonstrate that ATS systems are effective nutrient removal technologies, with 75% of evaluated locations achieving economic feasibility when nutrient credits are applied. However, only 29% of sites met the RFS threshold, underscoring the limitations of current biomass yields for large-scale fuel production. Despite these limitations, ATS systems demonstrate lower energy intensity compared to conventional nutrient removal methods and present a viable pathway for enhancing WWT sustainability. This work defines the benchmark for evaluating ATS systems in point-source applications, clearly demonstrating their value in water quality improvement while identifying key trade-offs in their role as biofuel platforms. By delivering the first integrated TEA-LCA of its kind, this study sets a precedent for rigorous, system-level assessment of emerging wastewater-to-resource technologies.

5. REFERENCES

[1] U. Epa, O. of Transportation, A. Quality, and S. Division, “Fast Facts: U.S. Transportation Sector Greenhouse Gas Emissions, 1990-2022 (EPA-420-F-24-022, May 2024),” 1990.

[2] Epa, “2023 Revision* to: Life Cycle and Cost Assessments of Nutrient Removal Technologies in Wastewater Treatment Plants,” 2021. Accessed: Mar. 25, 2025. [Online]. Available: https://www.epa.gov/system/files/documents/2023-06/life-cycle-nutrient-removal-2023-update.pdf

[3] S. H. Lee *et al.*, “Higher biomass productivity of microalgae in an attached growth system, using wastewater,” *J Microbiol Biotechnol*, vol. 24, no. 11, pp. 1566–1573, 2014, doi: 10.4014/jmb.1406.06057.

[4] D. T. Newby *et al.*, “Assessing the potential of polyculture to accelerate algal biofuel production,” *Algal Res*, vol. 19, pp. 264–277, Nov. 2016, doi: 10.1016/J.ALGAL.2016.09.004.

[5] K. Ullah *et al.*, “Algal biomass as a global source of transport fuels: Overview and development perspectives,” *Progress in Natural Science: Materials International*, vol. 24, no. 4, pp. 329–339, Aug. 2014, doi: 10.1016/J.PNSC.2014.06.008.

[6] B. T. Higgins and A. Kendall, “Life Cycle Environmental and Cost Impacts of Using an Algal Turf Scrubber to Treat Dairy Wastewater,” *J Ind Ecol*, vol. 16, no. 3, pp. 436–447, Jun. 2012, doi: 10.1111/j.1530-9290.2011.00427.x.

[7] J. Roostaei and Y. Zhang, “Spatially Explicit Life Cycle Assessment: Opportunities and challenges of wastewater-based algal biofuels in the United States,” *Algal Res*, vol. 24, pp. 395–402, Jun. 2017, doi: 10.1016/j.algal.2016.08.008.

[8] J. Liu, B. Pemberton, J. Lewis, P. J. Scales, and G. J. O. Martin, “Wastewater treatment using filamentous algae – A review,” *Bioresour Technol*, vol. 298, Feb. 2020, doi: 10.1016/j.biortech.2019.122556.

[9] A. B. Banks, P. H. Chen, C. Quiroz-Arita, R. W. Davis, and J. C. Quinn, “Geographically-resolved evaluation of the economic and environmental services from renewable diesel derived from attached algae flow-ways across the United States,” *Algal Res*, vol. 72, p. 103100, May 2023, doi: 10.1016/J.ALGAL.2023.103100.

[10] K. K. DeRose, R. W. Davis, E. A. Monroe, and J. C. Quinn, “Economic viability of proactive harmful algal bloom mitigation through attached algal growth,” *J Great Lakes Res*, vol. 47, no. 4, pp. 1021–1032, Aug. 2021, doi: 10.1016/j.jglr.2021.04.011.

[11] M. Kesaano and R. C. Sims, “Algal biofilm based technology for wastewater treatment,” *Algal Res*, vol. 5, no. 1, pp. 231–240, Jul. 2014, doi: 10.1016/J.ALGAL.2014.02.003.

[12] “HYDROMENTIA 2006 Suwannee-Prelim-Eng-Assessment-FINAL”. 2006. [Online]. Available: https://hydromentia.com/resources/ats-library/.

[13] J. M. Greene, D. Quiroz, B. J. Limb, and J. C. Quinn, “Geographically-Resolved Techno-Economic and Life Cycle Assessment Comparing Microalgae-Based Renewable Diesel and Sustainable Aviation Fuel in the United States,” *Environ Sci Technol*, Feb. 2025, doi: 10.1021/ACS.EST.4C06742/SUPPL_FILE/ES4C06742_SI_001.PDF.

[14] D. Quiroz, J. M. Greene, B. J. Limb, and J. C. Quinn, “Global Life Cycle and Techno-Economic Assessment of Algal-Based Biofuels,” *Environ Sci Technol*, vol. 57, no. 31, pp. 11541–11551, Aug. 2023, doi: 10.1021/acs.est.3c02892.

[15] M. Afshar and S. Mofatteh, “Biochar for a sustainable future: Environmentally friendly production and diverse applications,” *Results in Engineering*, vol. 23, p. 102433, Sep. 2024, doi: 10.1016/J.RINENG.2024.102433.

[16] S. Gurau, M. Imran, and R. L. Ray, “Algae: A cutting-edge solution for enhancing soil health and accelerating carbon sequestration – A review,” *Environ Technol Innov*, vol. 37, p. 103980, Feb. 2025, doi: 10.1016/J.ETI.2024.103980.

[17] K. Thiyagarasaiyar, B. H. Goh, Y. J. Jeon, and Y. Y. Yow, “Algae Metabolites in Cosmeceutical: An Overview of Current Applications and Challenges,” *Mar Drugs*, vol. 18, no. 6, p. 323, Jun. 2020, doi: 10.3390/MD18060323.

[18] J. Hoffman, R. C. Pate, T. Drennen, and J. C. Quinn, “Techno-economic assessment of open microalgae production systems,” *Algal Res*, vol. 23, pp. 51–57, Apr. 2017, doi: 10.1016/j.algal.2017.01.005.

[19] P. H. Chen and J. C. Quinn, “Microalgae to biofuels through hydrothermal liquefaction: Open-source techno-economic analysis and life cycle assessment,” *Appl Energy*, vol. 289, May 2021, doi: 10.1016/j.apenergy.2021.116613.

[20] K. DeRose, C. DeMill, R. W. Davis, and J. C. Quinn, “Integrated techno economic and life cycle assessment of the conversion of high productivity, low lipid algae to renewable fuels,” *Algal Res*, vol. 38, Mar. 2019, doi: 10.1016/j.algal.2019.101412.

[21] J. R. Cruce *et al.*, “Driving toward sustainable algal fuels: A harmonization of techno-economic and life cycle assessments,” *Algal Res*, vol. 54, p. 102169, Apr. 2021, doi: 10.1016/J.ALGAL.2020.102169.

[22] J. Barlow, R. C. Sims, and J. C. Quinn, “Techno-economic and life-cycle assessment of an attached growth algal biorefinery,” *Bioresour Technol*, vol. 220, pp. 360–368, Nov. 2016, doi: 10.1016/j.biortech.2016.08.091.

[23] S. J. Judd, F. A. O. Al Momani, H. Znad, and A. M. D. Al Ketife, “The cost benefit of algal technology for combined CO2 mitigation and nutrient abatement,” *Renewable and*

Sustainable Energy Reviews, vol. 71, pp. 379–387, May 2017, doi: 10.1016/J.RSER.2016.12.068.

[24] R. Davis, "BETO 2021 Peer Review: Algal Biofuels Techno-Economic Analysis 1.3.5.200," 2030.

[25] O. of Water, "Advanced Wastewater Treatment to Achieve Low Concentration of Phosphorus Advanced Treatment to Achieve Low Concentration of Phosphorus," 2007.

[26] B. J. Limb, J. C. Quinn, A. Johnson, R. B. Sowby, and E. Thomas, "The potential of carbon markets to accelerate green infrastructure-based water quality trading," *Commun Earth Environ*, vol. 5, no. 1, Dec. 2024, doi: 10.1038/s43247-024-01359-x.

[27] K. K. DeRose, R. W. Davis, E. A. Monroe, and J. C. Quinn, "Economic viability of proactive harmful algal bloom mitigation through attached algal growth," *J Great Lakes Res*, vol. 47, no. 4, pp. 1021–1032, Aug. 2021, doi: 10.1016/J.JGLR.2021.04.011.

[28] J. Clippinger and R. Davis, "Techno-Economic Assessment for Opportunities to Integrate Algae Farming with Wastewater Treatment," 2021, Accessed: Mar. 25, 2025. [Online]. Available: https://www.nrel.gov/docs/fy21osti/75237.pdf.

[29] "Estimated Total Nitrogen and Total Phosphorus Loads and Yields Generated within States | US EPA." Accessed: Mar. 25, 2025. [Online]. Available: https://www.epa.gov/nutrientpollution/estimated-total-nitrogen-and-total-phosphorus-loads-and-yields-generated-within

[30] A. Beattie *et al.*, "A probabilistic economic and environmental impact assessment of a cyanobacteria-based biorefinery," *Algal Res*, vol. 59, p. 102454, Nov. 2021, doi: 10.1016/J.ALGAL.2021.102454.

[31] J. M. Greene, D. Quiroz, S. Compton, P. J. Lammers, and J. C. Quinn, "A validated thermal and biological model for predicting algal productivity in large scale outdoor cultivation systems," *Algal Res*, vol. 54, Apr. 2021, doi: 10.1016/j.algal.2021.102224.

[32] D. Quiroz, J. M. Greene, J. McGowen, and J. C. Quinn, "Geographical assessment of open pond algal productivity and evaporation losses across the United States," *Algal Res*, vol. 60, p. 102483, Dec. 2021, doi: 10.1016/J.ALGAL.2021.102483.

[33] S. Kim *et al.*, "Application of attached algae flow-ways for coupling biomass production with the utilization of dilute non-point source nutrients in the Upper Laguna Madre, TX," *Water Res*, vol. 191, p. 116816, Mar. 2021, doi: 10.1016/J.WATRES.2021.116816.

[34] S. Jenkins, "Chemical Engineering Plant Cost Index Annual Average, Chem. Eng. ," https://www.chemengonline.com/2019-chemical-engineering-plantcost-index-annual-average/ .

[35] U.S. Bureau of Labor Statistics, “Producer Price Index by Commodity: Chemicals and Allied Products: Basic Inorganic Chemicals [WPU0613],” https://fred. stlouisfed.org/series/WPU0613. Accessed: Apr. 17, 2025. [Online]. Available: https://www.chemengonline.com/2019-chemical-engineering-plant-cost-index-annual-average/

[36] U.S. Bureau of Labor Statistics, “Employment, Hours, and Earnings from the Current Employment Statistics survey (National), Series ID: CEU3232500008,” https:// data.bls.gov/cgi-bin/srgate. Accessed: Apr. 17, 2025. [Online]. Available: https:// data.bls.gov/cgi-bin/srgate

[37] United States Department of Agriculture, “Fiscal Year 2019 USDA Budget Summary,” 2019. Accessed: Apr. 17, 2025. [Online]. Available: https://www.usda.gov/sites/default/files/documents/usda-fy19-budget-summary.pdf

[38] C. W. W. C. C. and T. R. S. Wiegand, “Cost of Urban Runoff Controls,” *American Society of Civil Engineers*, 1986.

[39] D. Knorr, J. Lukas, P. Schoen, and M. J. Biddy, “Production of Advanced Biofuels via Liquefaction Hydrothermal Liquefaction Reactor Design: April 5, 2013,” 2013. Accessed: Apr. 17, 2025. [Online]. Available: www.nrel.gov/publications.

[40] M. Marufuzzaman, S. D. Ekşioğlu, and R. Hernandez, “Truck versus pipeline transportation cost analysis of wastewater sludge,” *Transp Res Part A Policy Pract*, vol. 74, pp. 14–30, Apr. 2015, doi: 10.1016/J.TRA.2015.02.001.

[41] D. Hess, L. M. Wendt, B. D. Wahlen, J. E. Aston, H. Hu, and J. C. Quinn, “Techno-economic analysis of ash removal in biomass harvested from algal turf scrubbers,” *Biomass Bioenergy*, vol. 123, pp. 149–158, Apr. 2019, doi: 10.1016/J.BIOMBIOE.2019.02.010.

[42] R. Davis, J. Markham, C. Kinchin, N. Grundl, E. C. D. Tan, and D. Humbird, “Process Design and Economics for the Production of Algal Biomass: Algal Biomass Production in Open Pond Systems and Processing Through Dewatering for Downstream Conversion,” 2016. [Online]. Available: www.nrel.gov/publications.

[43] “ecoinvent Version 3.4.” Accessed: Apr. 10, 2025. [Online]. Available: https://support.ecoinvent.org/ecoinvent-version-3.4

[44] J. C. Bare, G. A. Norris, D. W. Pennington, and T. McKone, “TRACI: The tool for the reduction and assessment of chemical and other environmental impacts,” *J Ind Ecol*, vol. 6, no. 3–4, pp. 49–78, 2003, doi: 10.1162/108819802766269539/ABSTRACT.

[45] Intergovernmental Panel on Climate Change (IPCC), “The Earth’s Energy Budget, Climate Feedbacks and Climate Sensitivity,” in *Climate Change 2021 – The Physical*

Science Basis, Cambridge University Press, 2023, pp. 923–1054. doi: 10.1017/9781009157896.009.

[46] "U.S. Gasoline and Diesel Retail Prices." Accessed: Apr. 05, 2025. [Online]. Available: https://www.eia.gov/dnav/pet/pet_pri_gnd_dcus_nus_w.htm

[47] "Overview of the Renewable Fuel Standard Program | US EPA." Accessed: Apr. 05, 2025. [Online]. Available: https://www.epa.gov/renewable-fuel-standard-program/overview-renewable-fuel-standard-program

[48] A. K. Patel *et al.*, "Algae as an emerging source of bioactive pigments," *Bioresour Technol*, vol. 351, p. 126910, May 2022, doi: 10.1016/J.BIORTECH.2022.126910.

[49] Y. Wei *et al.*, "Hydrothermal liquefaction of municipal sludge and its products applications," *Science of The Total Environment*, vol. 908, p. 168177, Jan. 2024, doi: 10.1016/J.SCITOTENV.2023.168177.

[50] S. P. Singh and P. Singh, "Effect of temperature and light on the growth of algae species: A review," *Renewable and Sustainable Energy Reviews*, vol. 50, pp. 431–444, Oct. 2015, doi: 10.1016/J.RSER.2015.05.024.

[51] X. Gan, H. Klose, and D. Reinecke, "Optimizing nutrient removal and biomass production of the Algal Turf Scrubber (ATS) under variable cultivation conditions by using Response Surface Methodology," *Front Bioeng Biotechnol*, vol. 10, Sep. 2022, doi: 10.3389/fbioe.2022.962719.

[52] M. Hannon, J. Gimpel, M. Tran, B. Rasala, and S. Mayfield, "Biofuels from algae: challenges and potential," 2010.

[53] B. Siville and W. J. Boeing, "Optimization of algal turf scrubber (ATS) technology through targeted harvest rate," *Bioresour Technol Rep*, vol. 9, p. 100360, Feb. 2020, doi: 10.1016/J.BITEB.2019.100360.

[54] D. E. Berthold, K. G. Shetty, K. Jayachandran, H. D. Laughinghouse, and M. Gantar, "Enhancing algal biomass and lipid production through bacterial co-culture," *Biomass Bioenergy*, vol. 122, pp. 280–289, Mar. 2019, doi: 10.1016/J.BIOMBIOE.2019.01.033.

[55] W. H. , C. L. and K. Jensen. R. Adey, "Phosphorus Removal from Natural Waters," no. Ecol. 1: 29-39, 1993, Accessed: Apr. 13, 2025. [Online]. Available: https://hydromentia.com/wp-content/uploads/2015/06/1993_Adey-et-al-Phosphorus-Removal-from-Natural-Waters.pdf

[56] B. J. Furnish and T. A. Keller, "Carbon limitation in hypereutrophic, periphytic algal wastewater treatment systems," *PLoS One*, vol. 15, no. 10, p. e0240525, Oct. 2020, doi: 10.1371/JOURNAL.PONE.0240525.

APPENDIX A

A.1 Supplementary Figures

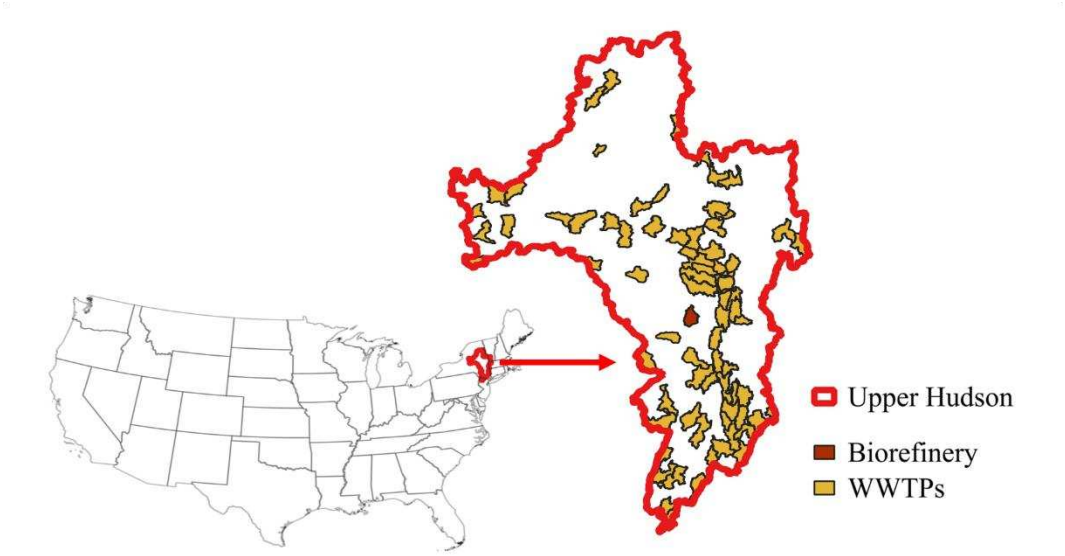

Figure A1. Upper Hudson, a hydraulic unit code 6 (HUC6) basin, identified on the map of the continental United States. Inset: a zoomed-in view of the HUC6 region showing the locations of wastewater treatment plants and biorefinery.

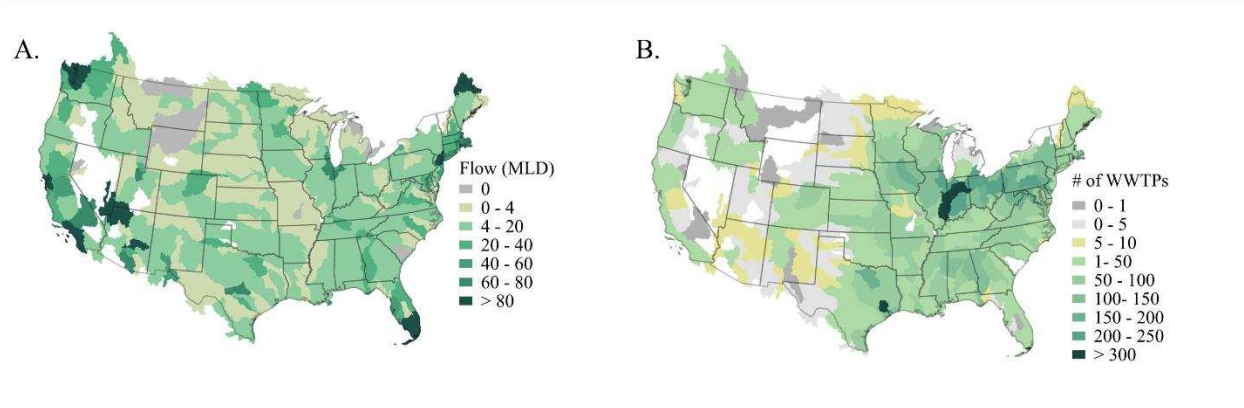

Figure A2. A) Average flow of each Hydraulic Unit Code (HUC) 6 in million liters per day (MLD) across continental united states (CONUS). B) Number of wastewater treatment plants (WWTP) considered in this study for each HUC6 across CONUS. A HUC12 location in Maine was omitted in this study for having too high of flow that was an outlier within that HUC6 region.

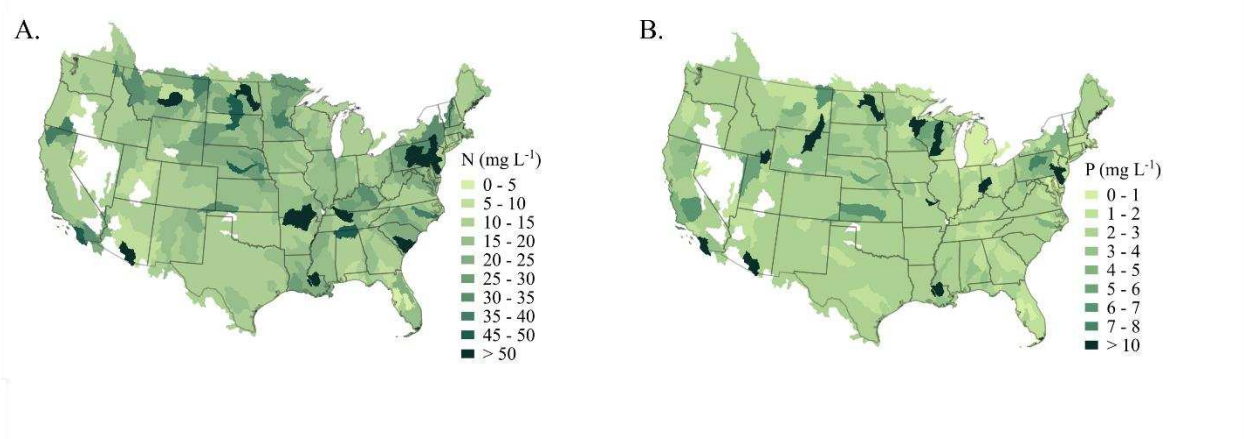

Figure A3. A) Average of the concentration of nitrogen (N) in the effluent of each wastewater treatment plant (WWTP) in each Hydraulic Unit Code 6 (HUC6). B) Average concentration of phosphorus (P) in the effluent of each WWTP in each HUC6.

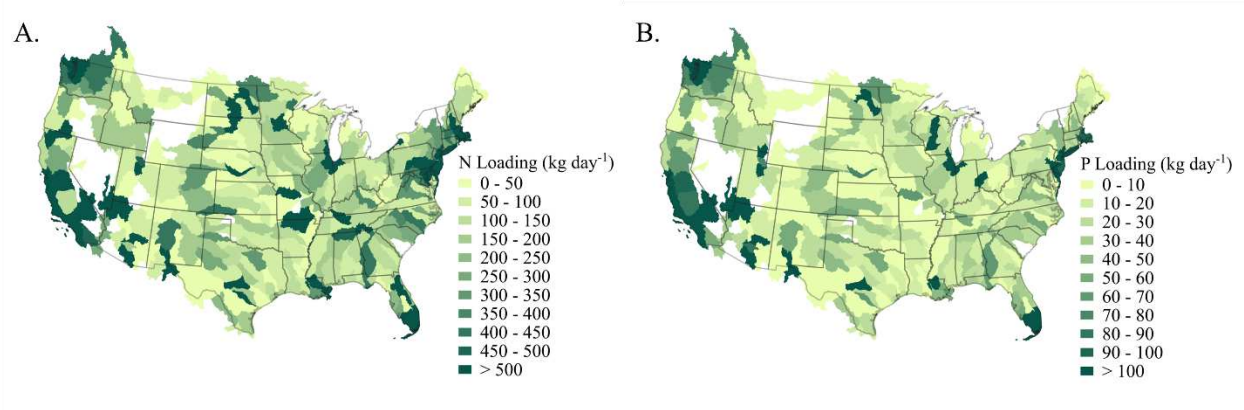

Figure A4. A) Average of the nutrient loadings for nitrogen (N) of each wastewater treatment plant (WWTP) in each Hydraulic Unit Code 6 (HUC6). B) Average nutrient loadings for phosphorus (P) of each WWTP in each HUC6. White areas in both maps represent regions with missing nutrient data or zero wastewater flow.

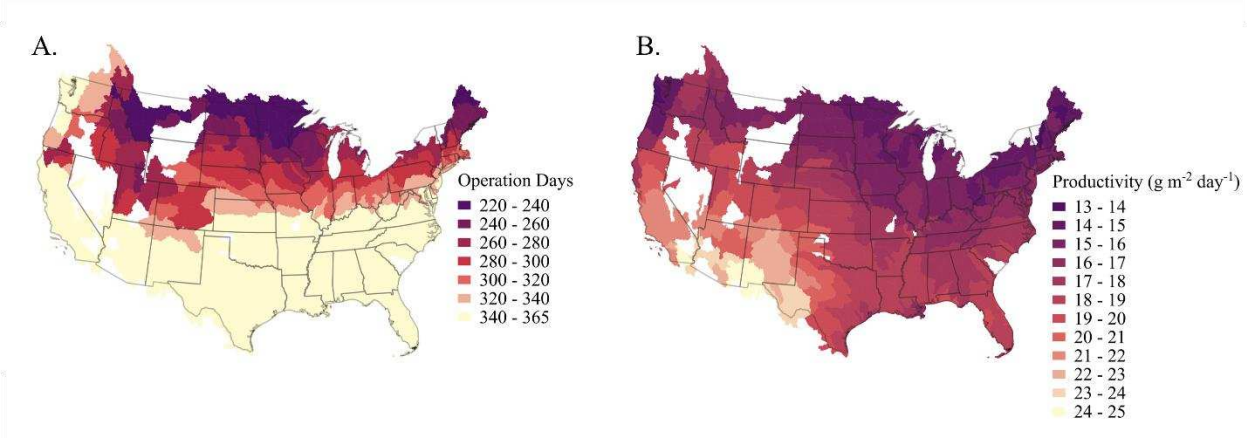

Figure A5. A) Operational days of each Hydraulic Unit Code 6 (HUC6) based off of number of freezing events. B) Productivity in each HUC6 based on global horizontal irradiance and light efficiency of the algae. White areas in both maps represent regions with missing nutrient data or zero wastewater flow.

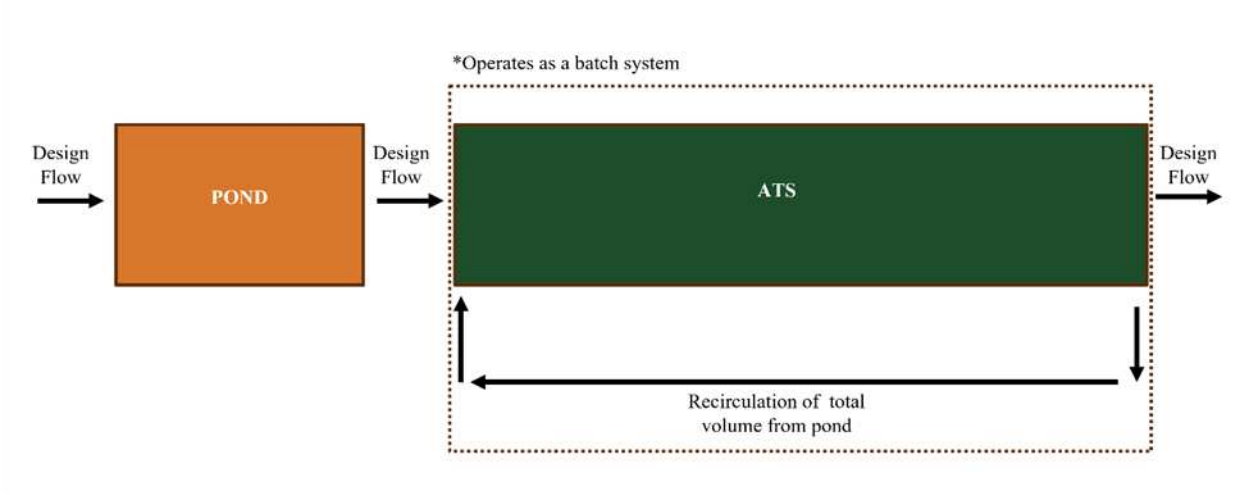

Figure A6. Diagram of algal turf scrubber (ATS) treatment process. ATS treatment system includes the flow-way and tanks to support the recirculation process. The total volume of the pond enters the ATS system and recycles. The ATS system is scaled to complete the required cycles in a day.

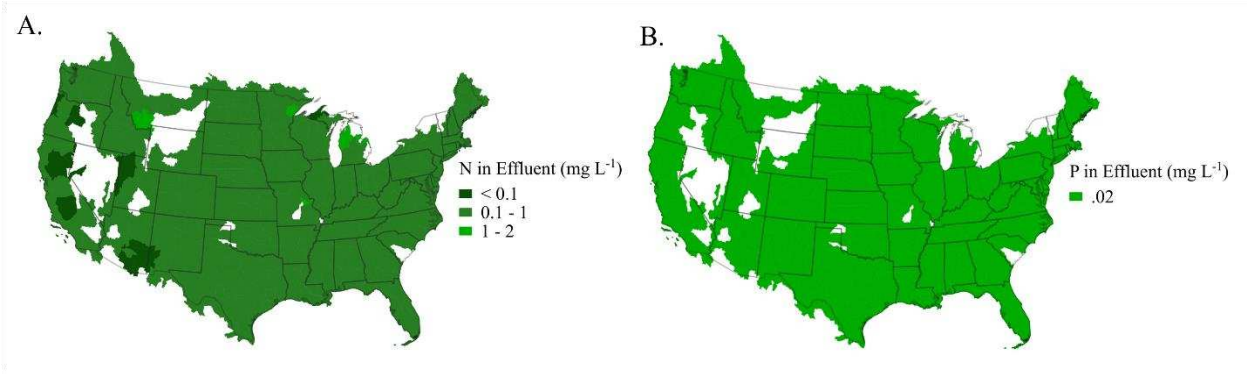

Figure A7. A) Average of the nutrient loadings for nitrogen (N) of each wastewater treatment plant (WWTP) in each Hydraulic Unit Code 6 (HUC6). B) Average nutrient loadings for phosphorus (P) of each WWTP in each HUC6. White areas in both maps represent regions with missing nutrient data or zero wastewater flow.

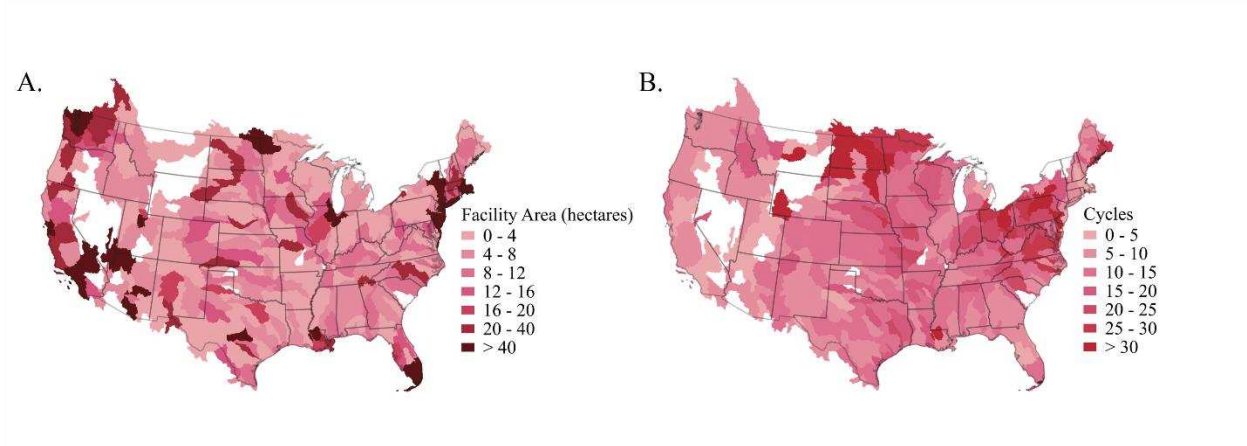

Figure A8. A) Average facility area of the algal turf scrubber treatment (ATS) system for each Hydraulic Unit Code 6 (HUC6) across continental United States (CONUS). B) Average cycles required for the ATS system for each HUC6 across CONUS. A and B present the required area and cycles to treat wastewater treatment effluent to EPA Level 5 targets of 2 mg L^{-1} for total nitrogen and 0.02 mg L^{-1} for total phosphorus. White areas in both maps represent regions with missing nutrient data or zero wastewater flow.

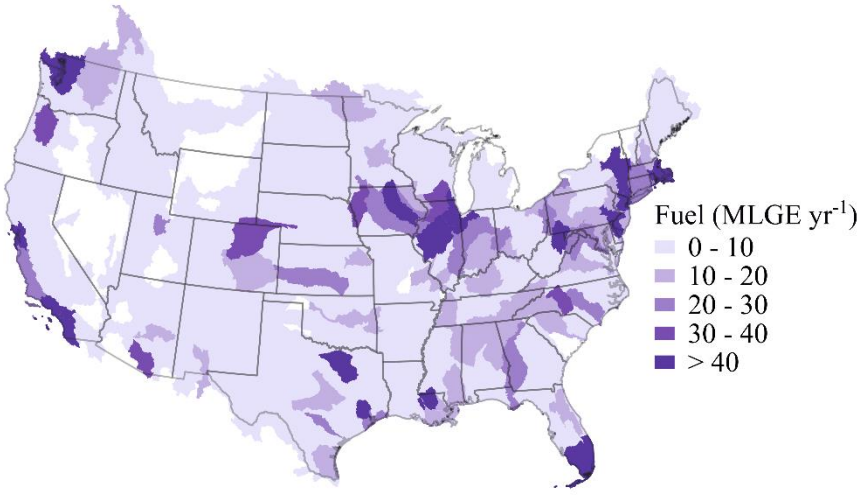

Figure A9. Fuel produced from biorefineries located in each hydraulic unit code 6 across the continental United States shown in million liters of gasoline equivalent per year (MLGE yr^{-1}). White areas in both maps represent regions with missing nutrient data or zero wastewater flow.

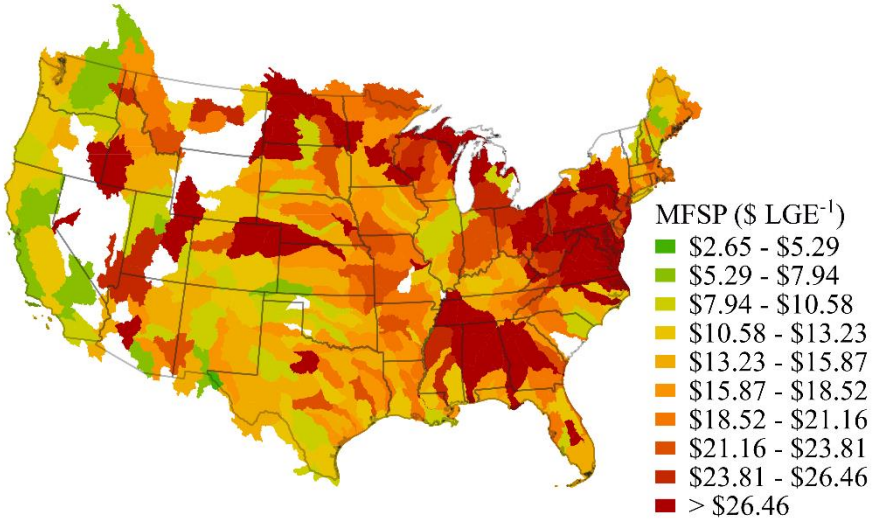

Figure A10. Minimum fuel selling price (MFSP) in dollars per liters of gasoline equivalent ($ LGE^{-1}) for each hydraulic unit code 6 across the continental united states. White areas in both maps represent regions with missing nutrient data or zero wastewater flow.

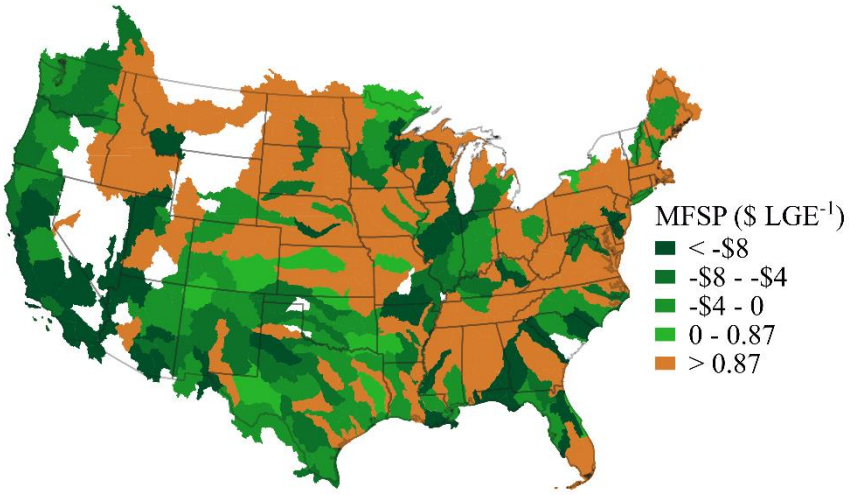

Figure A11. Minimum fuel selling price (MFSP) in dollars per liters of gasoline equivalent ($ LGE^{-1}) with a nutrient credit of \$30 kg^{-1} for nitrogen and \$225 kg^{-1} for phosphorus, for each hydraulic unit code 6 across the continental united states. White areas in both maps represent regions with missing nutrient data or zero wastewater flow.

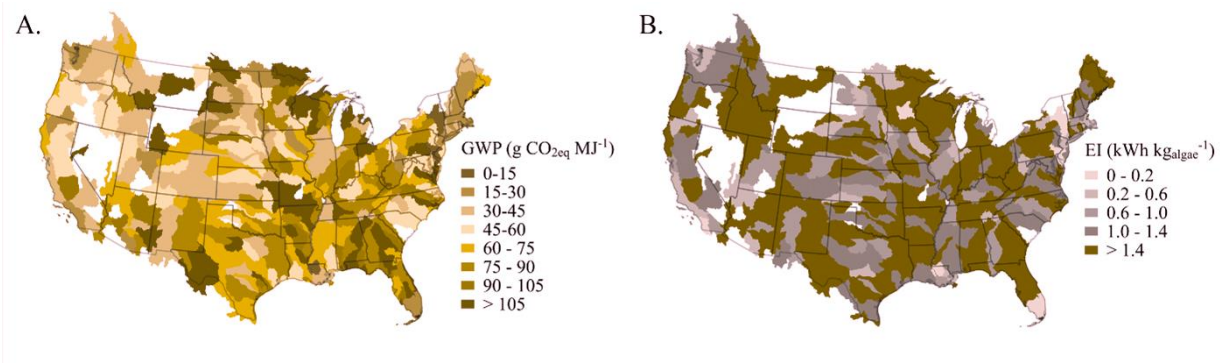

Figure A12. A) Net global warming potential (GWP) across the continental United States (CONUS) for each Hydrological Unit Code 6 (HUC6) basin. B) Electricity intensity of Algal Turf Scrubber systems aggregated to a HUC6 basin level across CONUS, expressed in kilowatt-hours per kilogram of ash free dry biomass produced (kWh kg_{algae}^{-1}). White areas in both maps represent regions with missing nutrient data or zero wastewater flow.

A.2 Process Model Equations

Equation A1. Productivity Calculation [1]

$$\text{prod} = \text{GHI} * \frac{86400\ \text{s}}{1\ \text{day}} * \frac{1\ \text{kJ}}{1000\text{J}} * \text{GHI\_PAR} * \text{light}_{\text{eff}} * \frac{1}{\text{energy density}}$$

Where:

prod = productivity of biomass; g m^{-2} day^{-1}

GHI = global horizontal irradiance; W m^{-2}

GHI_PAR = 0.458; (kJ m^{-2} day^{-1} PAR)(kJ m^{-2} day^{-1} GHI)$^{-1}$

$\text{light}_{\text{eff}}$ = 2.8; %

energy density = 22; kJ g^{-1}

Equation A2. Electricity Equation

$$\text{pumping power} = \left(\text{flow} * 2 * \text{pump}_{\text{energy}} * \frac{24\ \text{hr}}{1\ \text{day}}\right) - \left(\frac{\text{flow}}{\text{cycles}} * \text{pump}_{\text{energy}} * \frac{24\ \text{hr}}{1\ \text{day}}\right)$$

Where:

pumping power = electricity use of the algal turf scrubber to pump water through the system

flow = $\text{MLD} * 10^6 * \frac{1\ \text{m}^3}{1000\ \text{L}}\ \ \frac{1\ \text{day}}{24\ \text{hr}} * \text{cycles}$; m^3 hr^{-1}

MLD = design flow of the WWTP in million liters per day

cycles = Number of times the volume of water needs to pass through the system in one day

$\text{pump}_{\text{energy}}$ = 0.0267kWh m^{-3}

A.3 Media Recipe

Table A1. Media recipe.

NaNO3 (mg/L)	91.00
KH2PO4 (mg/L)	6.59
MgSO4*7H2O (mg/L)	202.73
CaCl2*2H2O (mg/L)	167.20
NaHCO3 (mg/L)	82.61
L1 Bigelow Trace Metals (mL)	0.10
L1 Bigelow vitamin solution (mL)	0.05

A.4 HTL Model Input Table

Table A2. Inputs to downstream processing model.

Parameter	**Value**	**Units**	**Reference**
Ash Reduction Inputs			
Filter Press Power Requirement	1350	kJ m^{-3}	[2]
De-ash Reaction Time	24	hr	[2]
HTL Inputs			
Annual Uptime	330	days	[3]
Proteins	0.52	% of solids	[2]
Carbohydrates	0.31	% of solids	[2]
Lipids	0.05	% of solids	[2]
Ash	0.12	% of solids	[2]
Hydrogen	84.87	kg (metric ton biocrude)$^{-1}$	[3]
Natural Gas	7.82	kg (metric ton biocrude)$^{-1}$	[3]
Process Water	2387.06	kg (metric ton biocrude)$^{-1}$	[3]
Grid Electricity	0.48	kW (metric ton biocrude)$^{-1}$	[3]
Biocrude Yield	0.35	% solids	[3], [4]
Aqueous Phase Yield	0.24	% solids	[3], [4]
Solids Yield	0.12	% solids	[3], [4]
Gas Yield	0.16	% solids	[3], [4]
Diesel Yield	66%	% biocrude	[3]

Naphtha Yield	13%	% biocrude	[3]
Land Scaling Value	1.52		[5]
Residence Time	30	min	[3]
Reaction Temperature	350	℃	[3]
Reactor Diameter	0.203	m	[3]
Biochar Recovery	60	%	[3]
NH3EQ Recovery	60	%	[3]
DAPEQ Recovery	60	%	[3]

A.5 Costing Tables

Table A3. BETO Nth of a kind plant costing assumptions.

Parameter	Value
Internal Rate of Return	10%
Plant Financing (Debt)	60% of Total Capital Cost
Plant Financing (Equity)	40% of Total Capital Cost
Plant Life	30 years
Income Tax Rate	35%
Interest Rate for Debt Financing	8% annual
Loan Term	10 years
Working Capital Cost	5% of Capital Cost (Excluding Land)
Depreciation Schedule	7 years MACRS schedule
Construction Period, Year -2	8% completed construction
Construction Period, Year -1	60% completed construction
Construction Period, Year 0	32% completed construction
Plant Salvage Value	None
Startup Time	6 months
Startup Capacity	50%

Table A4. Cost assumptions for cultivation model.

Cultivation Costing			
Parameter	**Value**	**Units**	**Reference**
CAPEX			
Direct Costs			
Land Cost	11,032	$/hectare	[6]
Tank Cost	7.75(V)^0.75	$	[7]
Growth System	155,321	$/hectare	[8]
Harvest Equipment	17,649	$/hectare	[8]
Peripheral	50	% of growth system costs	[9]
Warehouse	4	% peripheral and growth system costs	[9]
Site Development	9	% peripheral and growth system costs	[9]
Piping	5	% peripheral and growth system costs	[9]
Indirect Costs			
Prorateable Expenses	10	% direct costs without land	[9]
Field Expenses	10	% direct costs without land	[9]
Home Office and Construction	20	% direct costs without land	[9]
Project Contingency	10	% direct costs without land	[9]
Working Capital	5	% of total CAPEX	
OPEX			
Labor	4,185	$/hectare	[8]
Harvest	1,933	$/hectare	[8]
Maintenance	1.60	% of capex	[8]

*All costing projected to 2024 dollars

Table A5. Cost assumptions for downstream processing.

HTL Costing						
Parameter	**Value**	**Units**	**Cost year**	**Reference**	**Scaling value**	**Units**
CAPEX						
Ash reduction						
De-ash Tank	0.16	mill $	2005	[1]	1	unit
Filter Press	0.01	mill $	2010	[1]	98	$m^3\ hr^{-1}$
De-ash Pumps	0.04	mill $	2010	[1]	45881	kg hr^{-1}
HTL						
First feed preheater	44.60	mill $	2012	[10]	49756	ft^2
Second feed preheater	31.86	mill $	2012	[10]	35540	ft^2
Feed recycle heat exchanger	2.95	mill $	2012	[10]	4500	ft^2
Final feed heater	1.00	mill $	2012	[10]	6032	ft^2
HTL reactor	0.27	mill $	2013	[10]	480	ft
Reactor gas KO drum	5.60	mill $	2012	[10]	1719856	Lb hr^{-1}
Solids filter	1.31	mill $	2011	[10]	3689	gpm
Separator	3.57	mill $	2011	[10]	3689	gpm
Bio-oil heat recovery steam generator	0.10	mill $	2012	[10]	868	ft^2
Upgrading						
Hydrotreater reactor, vessels, columns	27.00	mill $	2007	[10]	6524	bpd
Hydrogen compressor	1.39	mill $	2011	[10]	17.1	MMscfd H2
Hydrogen recycle PSA	1.75	mill $	2004	[10]	17.1	MMscfd H2
Hydrocracker unit and auxiliaries	25.00	mill $	2007	[10]	2200	bpd
Utilities						
Hot oil system package	1.20	mill $	2012	[10]	60	MMBTU hr^{-1}
Hot oil	2.10	mill $	2012	[10]	52400	gal hot oil
Cooling tower system	2.00	mill $	2009	[10]	35631668	Lb hr^{-1}
Cooling water pump	0.45	mill $	2009	[10]	35631668	Lb hr^{-1}
Plant air compressor	0.03	mill $	2002	[10]	2000	t/d

Hydraulic truck dump with scale	0.08	mill $	1998	[10]	2000	t/d
Firewater pump	0.18	mill $	1997	[10]	2000	t/d
Instrument air dryer	0.01	mill $	2002	[10]	2000	t/d
Plant air receiver	0.01	mill $	2002	[10]	2000	t/d
Firewater storage tank	0.17	mill $	1997	[10]	2000	t/d
HTL oil intermediate storage (3 day)	0.47	mill $	2005	[10]	1056846	gal
Naphtha storage (3 day)	0.32	mill $	2005	[10]	558000	gal
Biodiesel storage (3 day)	0.32	mill $	2005	[10]	558000	gal
OPEX						
Feedstock	MBSP	$ kg^{-1}				
Natural Gas	0.23	$ $MMBTU^{-1}$	2011	[11]		
Electricity	0.801	$ kWh^{-1}	2024	[12]		
Cooling water	0.00	$ kg^{-1}	2011	[11]		
Hydrogen	1.57	$ kg^{-1}	2012	[13]		
Solids disposal	0.03	$ kg^{-1}		[14]		
Labor	1.42	mill $ $year^{-1}$		[3]	2025	hectares
Benefits and Overhead	90%	% Salaries		[3]		
Maintenance	3%	% ISBL		[3]		
Property Insurance	1%	% FCI		[3]		
Transportation	0.058	$ $mile^{-1}$ m^{-3}	2015	[15]		
NH3EQ Value	0.39	$ kg^{-1}	2011	[5]		
DAPEQ value	0.32	$ kg^{-1}	2012	[5]		

A.6 Sensitivity Analysis

Figure A13. Sensitivity analysis of cultivation model.

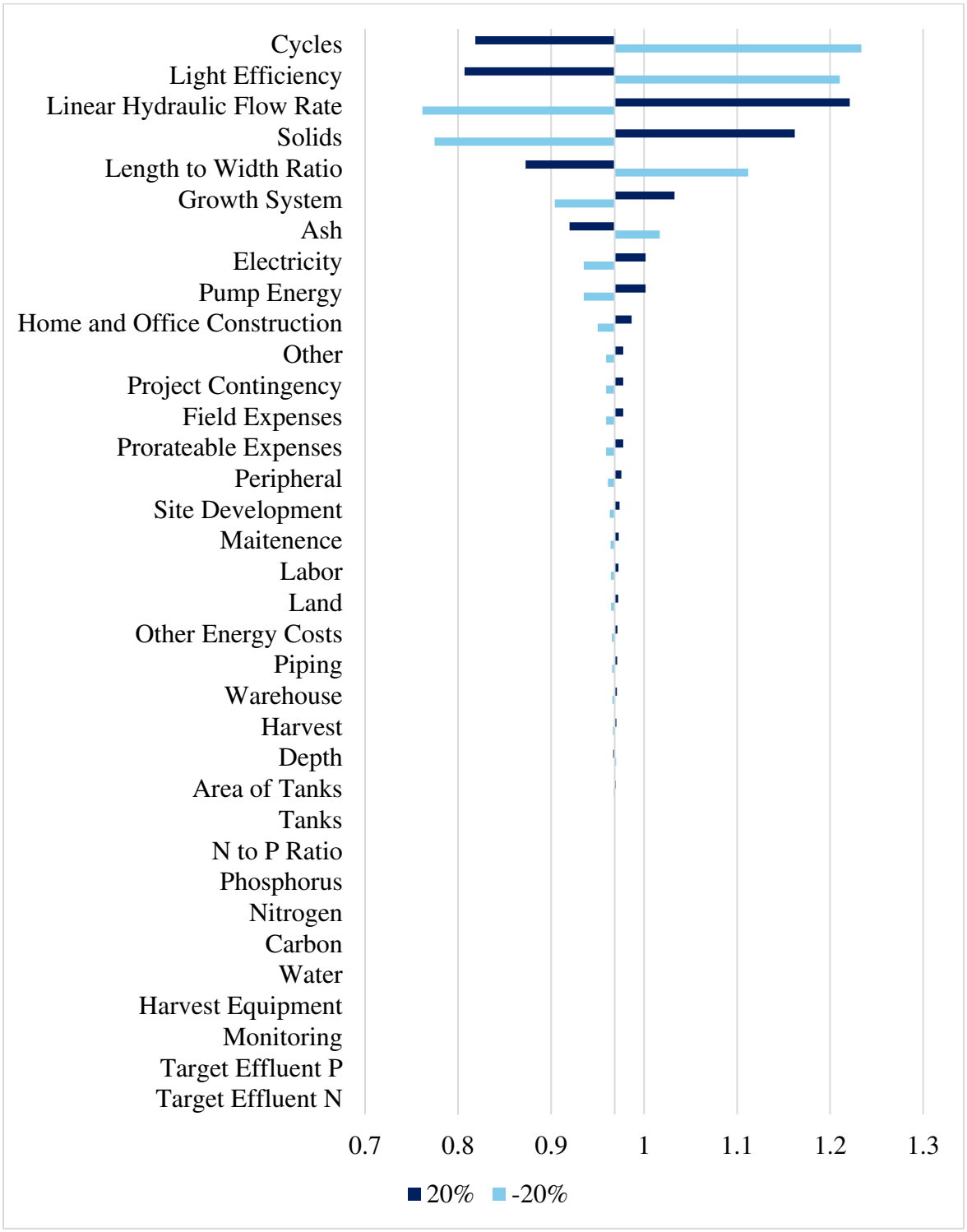

A.7 References

[1] A. B. Banks, P. H. Chen, C. Quiroz-Arita, R. W. Davis, and J. C. Quinn, "Geographically-resolved evaluation of the economic and environmental services from renewable diesel derived from attached algae flow-ways across the United States," *Algal Res*, vol. 72, p. 103100, May 2023, doi: 10.1016/J.ALGAL.2023.103100.

[2] K. DeRose, C. DeMill, R. W. Davis, and J. C. Quinn, "Integrated techno economic and life cycle assessment of the conversion of high productivity, low lipid algae to renewable fuels," *Algal Res*, vol. 38, Mar. 2019, doi: 10.1016/j.algal.2019.101412.

[3] P. H. Chen and J. C. Quinn, "Microalgae to biofuels through hydrothermal liquefaction: Open-source techno-economic analysis and life cycle assessment," *Appl Energy*, vol. 289, May 2021, doi: 10.1016/j.apenergy.2021.116613.

[4] S. Jones *et al.*, "Process Design and Economics for the Conversion of Algal Biomass to Hydrocarbons: Whole Algae Hydrothermal Liquefaction and Upgrading," 2014. [Online]. Available: http://www.osti.gov/bridge

[5] R. Davis, J. Markham, C. Kinchin, N. Grundl, E. C. D. Tan, and D. Humbird, "Process Design and Economics for the Production of Algal Biomass: Algal Biomass Production in Open Pond Systems and Processing Through Dewatering for Downstream Conversion," 2016. [Online]. Available: www.nrel.gov/publications.

[6] United States Department of Agriculture, "Fiscal Year 2019 USDA Budget Summary," 2019. Accessed: Apr. 17, 2025. [Online]. Available: https://www.usda.gov/sites/default/files/documents/usda-fy19-budget-summary.pdf

[7] C. W. W. C. C. and T. R. S. Wiegand, "Cost of Urban Runoff Controls," *American Society of Civil Engineers*, 1986.

[8] K. K. DeRose, R. W. Davis, E. A. Monroe, and J. C. Quinn, "Economic viability of proactive harmful algal bloom mitigation through attached algal growth," *J Great Lakes Res*, vol. 47, no. 4, pp. 1021–1032, Aug. 2021, doi: 10.1016/j.jglr.2021.04.011.

[9] R. Davis *et al.*, "Economic, Greenhouse Gas, and Resource Assessment for Fuel and Protein Production from Microalgae: 2022 Algae Harmonization Update Contributing Authors Report Coordination: Algae Farm TEA: HTL Conversion TEA: System LCA," 2024, Accessed: Apr. 17, 2025. [Online]. Available: www.nrel.gov/publications.

[10] D. Knorr, J. Lukas, P. Schoen, and M. J. Biddy, "Production of Advanced Biofuels via Liquefaction Hydrothermal Liquefaction Reactor Design: April 5, 2013," 2013. [Online]. Available: www.nrel.gov/publications.

[11] A. Dutta *et al.*, “Process Design and Economics for Conversion of Lignocellulosic Biomass to Ethanol: Thermochemical Pathway by Indirect Gasification and Mixed Alcohol Synthesis,” May 2011, doi: 10.2172/1015885.

[12] “Electric Power Monthly - U.S. Energy Information Administration (EIA).” Accessed: Mar. 25, 2025. [Online]. Available: https://www.eia.gov/electricity/monthly/epm_table_grapher.php?t=epmt_5_6_a

[13] R. T. M. M. Dillich S, “Hydrogen Production Cost Using Low-Cost Natural Gas. ,” *DOE Hydrog. Fuel Cells Progr. Rec.* , pp. 3–8, 2013.

[14] R. Davis *et al.*, “Process Design and Economics for the Conversion of Algal Biomass to Biofuels: Algal Biomass Fractionation to Lipid- and Carbohydrate-Derived Fuel Products,” 2013. [Online]. Available: www.nrel.gov/publications.

[15] M. Marufuzzaman, S. D. Ekşioğlu, and R. Hernandez, “Truck versus pipeline transportation cost analysis of wastewater sludge,” *Transp Res Part A Policy Pract*, vol. 74, pp. 14–30, Apr. 2015, doi: 10.1016/J.TRA.2015.02.001.